CALIBRATION OF THE HIGH ENERGY TELESCOPES FOR THE VOYAGER AND ISEE COSMIC RAY EXPERIMENTS

Volume 3

Prepared for
GODDARD SPACE FLIGHT CENTER

By
COMPUTER SCIENCES CORPORATION

Under

Contract No. NAS 5-24350
Task Assignment 721

Prepared by:

P. Schuster 3/7/83
P. Schuster Date

J. H. Baumert 3/7/83
Dr. J. Baumert Date

Reviewed by:

E S Munday 3/7/83
E. Munday Date
Section Manager

Approved by:

Mac D Silberg 3/7/83
M. Silbergeld Date
Department Manager

M. Plett 3/9/83
Dr. M. Plett Date
Project Manager

ABSTRACT

The High Energy Telescopes (HETs) of the Cosmic Ray experiments on board the Voyager-1 and -2, and ISEE-3 spacecraft measure charged particle fluxes of about 1-500 MeV per nucleon for nuclei with atomic numbers of 1-28. This volume describes the steps in the calibration of the experimental data from the ISEE-3 spacecraft and the procedures to be followed in using the calibration software.

TABLE OF CONTENTS

LIST OF ILLUSTRATIONS

LIST OF TABLES

SECTION 1 - INTRODUCTION TO VOLUME 3

This document describes the calibration work for the High Energy Telescopes (HETs) onboard the ISEE-3 (International Sun-Earth Explorer) spacecraft. This calibration process for the HETs consists of constructing a computer model of each telescope using known detector thicknesses and spacings, and then comparing it to selected data in an iterative fashion until the model is deemed accurate enough.

There are three main activities which are necessary to calibrate the data:

1. Produce MATRIX plots for mass lines of interest. From these
   a. determine endpoints in channel units and
   b. delineate tracks for the response mode tables.
2. Use range/energy theory incorporated in existing computer programs and geometry factor calculation to assign energies and geometries to the tracks delineated in 1b. Then
   a. create and edit the response mode data where needed, and
   b. enter the mode into the ISEE calibration data catalog.
3. Execute the FLUXPLOT program summarizing energy subregions within the various response modes. The resulting fluxes are compared with other data in order to achieve maximum self-consistency in the data.

This self-consistency is achieved by varying in an iterative way the MeV/channel, the offset, and possibly the detector model thicknesses.

The implementation of these activities is described in Calibration of the High Energy Telescopes for the Voyager and ISEE Cosmic Ray Experiments (Volumes 1 and 2)

(References 1 and 2). The discussion in this volume assumes that the reader is familiar with the material in Volumes 1 and 2. The work was done in two segments. One segment, the stopping particle calibration, was performed by Dr. Don Reames. The other segment, the penetrating particle calibration, was done by Dr. Frank McDonald.

For the stopping particle work the pre-flight calibration FSMeV and OFFSET values were used as first estimates of those parameters. TESTA and BOXGEN were used to generate the complete TRACKs with energies and geometry factors for all modes. TRACKs were made with the use of the box-spread factor and mass-line overlay priority parameters in BOXGEN. An iterative process was applied in which the shape of each species' computer TRACK was made to overlay the data mass lines, while requiring self-consistency in other mass-line TRACK overlays.

The penetrating particle calibration procedures were the same as used for Voyager-2 (as described in Volume 2 of this document). Initial Full Scale MeV (FSMeV) parameters were taken from the stopping particle calibration work. The Sum C detector OFFSETS were made equal to zero. In subsequent calibration iterations, the FSMeV and offset parameters were adjusted to give self-consistency in the flux data. The programs TESTM and BIGNEW were used to generate the energies and geometry factors for the penetrating event TRACKs. The actual TRACKs were hand-delineated using MATRIX program output.

In the penetrating particle calibration work, fluxes from HET-2 could not be made self-consistent with HET-1. HET-1 was selected as the reliable HET, and penetrating response results are given for that HET only.

The work sources used in producing the current response mode tables are summarized in Table 1.

Table 1 Origin of Response Modes for ISEE-3

	TRACK	Energies	Geometry Factors
2-D stopping<1>	BOXGEN	BOXGEN	BOXGEN
	TESTA	TESTA	TESTA
3-D stopping<1>	BOXGEN	BOXGEN	BOXGEN
	TESTA	TESTA	TESTA
all penetrating	hand	BXGNEW<+>	BXGNEW<+>
		TESTM	TESTM

<1> these are as done by Reames' work
<+> detector description files in Tables 6 - 7 were used.

This document is divided into four sections as follows: Sections 2 and 3 describe the MATRIX program information used and the generation of response mode tables for the penetration calibration work. Section 4 summarizes flux results for the current calibration responses for protons and alpha particles. Appendix E briefly summarizes the stopping particle work.

In closing, the computer printout books mentioned below include the stopping particle TESTA ,BOXGEN, and INSTALC output in the book ISEE-3 CALIBRATION: I1; the penetrating mode MATRIX program data in the book ISEE-3 CALIBRATION: I2; the PDP11/70 output from TESTM and BXGNEW in the book ISEE-3 CALIBRATION: I3; and the FLUXPLOT results in book ISEE-3 CALIBRATION: I4. A log starting in August 1982 is maintained for all changes and/or additions to the CATALOG.DATA dataset.

SECTION 2 - MATRIX PROGRAM INFORMATION FOR PENETRATING RESPONSES

In the penetrating response work the maximum pulse height, or endpoint, is determined from a set of two-dimensional plots (matrix plots), which display the number of events as a function of the pulse heights in two detector sets. This section discusses the determination of endpoints.

2.1 DETERMINATION OF ENDPOINTS AND TRACK DEFINITIONS

2.1.1 ENDPOINTS

The different particle mass lines are located by producing plots of the various possible experiment event types. These plots are produced by the program MATRIX. Table 2 lists the possible ISEE-3 event types along with the electronic coincidence logic constraint for that data type. The plots are produced customarily for a selected time period.

For the Voyager and ISEE-3 experiments, the convention is to sum the y-axis channel counts over the track width for each x-axis channel near the endpoint and to plot the result on semi-log paper. The x-axis channel where the number of counts falls to approximately one-half of the maximum is taken to be the endpoint. Examples of MATRIX plots used for endpoint determination are presented in Appendix A for alpha and proton particles, high and low gain, three-dimensional

Table 2 Event-Type Summary for ISEE-3

event type		coincidence logic equation
5	-	IAS(A1.A2.¬C4.¬G1.¬G2)
6	-	IASZ3(A1.A2.SA.¬C4.¬G3)
7	-	IBSP(B1.B2.SE.¬C1.¬G1.¬G2)
8	-	IBSE(B1.B2.C4.¬SB.¬C1.¬G1)
9	-	IBSZ2(B1.B2.SB.¬C1.¬G3)
10	-	IPENH(B1.B2.C1)
11	-	IPENL(B1.B2.C1)
12	-	IIAS(A1.A2.¬C4.¬G1.¬G2)
13	-	IIASZ3(A1.A2.SA.¬C4.¬G3)
14	-	IIBSP(B1.B2.SE.¬C1.¬G1.¬G2)
15	-	IIBSE(B1.B2.C4.¬SB.¬C1.¬G1)
16	-	IIBSZ2(B1.B2.SE.¬C1.¬G3)
17	-	IIPENH(B1.B2.C1)
18	-	IIPENL(B1.B2.C1)
19	-	Vlet I event type 0
20	-	Vlet I event type 1
21	-	Vlet II event type 0
22	-	Vlet II event type 1

stopping events.

The channel endpoint determinations for the Sum C detectors were done by Dr. F. McDonald. The MATRIX program was run for the dates given in Appendix A.

2.1.2 TRACK DEFINITIONS

Track definitions are needed to generate response matrices. These definitions are provided in MATRIX program information.

Two and three-dimensional stopping mode TRACK overlays were generated by Dr. D. Reames with the programs TESTA and BOXGEN and were entered into the CATALOG.DATA dataset. Appendix B gives an expanded summary of that TRACK definition work.

Penetrating mode TRACKS were defined by Dr. F. McDonald. Matrix program requests for penetrating mode data are shown in Table 3 and representative input cards are listed in Table 4. Appendix C shows the output TRACK data for the low gain B uni-directional penetrating track definition for alpha particles. These figures are representative of typical penetrating event tracks. The time period used for the ISEE-3 HETs is listed in Table 3. A compilation of these data can be found in the bound calibration computer printout documentation book ISEE-3 CALIBRATION: 12.

2.1.3 EXECUTING THE MATRIX PROGRAM

Job Control Language (JCL) for running MATRIX program on the IBM 3081 is found in GSFC.LIB.CNTL(MATRIX). A data deck similar to that in Table 4 must be appended to the JCL. This example is for HET-1 high gain proton bi-directional tracks.

A userguide for the MATRIX program exists in SB#IC.USERGIDE.TEXT(MATRIX).

Table 3 Matrix Program Requests for Penetrating Track Definitions

Penetrating Modes

Particle	Event	Type	Detectors Plotted	Restrictions on Plot/ + compression	Response Mode
Alpha	10	B-pen	B1 vs C1	(-G2).-(G1.-G3). CMP=1 SUMC= 31-110, by 2 CMP=1 SUMC= 90-170, by 4 CMP=2 SUMC=157-220, by 4	IPH,IPY
Alpha	10	A-pen	"	" "	IPZ
Proton	10	B-pen	B1 vs C1	CMP=1 SUMC=1-60	IPH,IPY
Proton	10	A-pen	"	" "	IPZ
Alpha lowq	11	B-pen	B1 vs C1	tag as for IPH alpha CMP=1 SUMC=15-50, by 2 CMP=1 SUMC=1-15, by 1	IP,IPB
Alpha lowq	11	A-pen	"	" "	IPA
Alpha	17	B-pen	B1 vs C1	(-G2).-(G1.-G3). as for HET I	IIPH,IIPY
Alpha	17	A-pen	"	" "	IIPZ
Proton	17	B-pen		as for HET I	IIPH,IIPY
Proton	17	A-pen	"	" "	IIPZ
Alpha lowq	18	B-pen	B1 vs C1	as for IPH alpha CMP=1 SUMC=15-50, by 2 CMP=1 SUMC=1-15, by 1	IIP,IIPB
Alpha lowq	18	A-pen	"	" "	IIPA

HET 1 and 2 data times: 78/11/23 - 79/02/16
(exclude 78/12/10 - 78/12/16
78/12/30 - 79/01/01
79/01/21 - 79/01/23

The tags : (-G2).-(G1.-G3). are set for all events

Table 4   Sample Card Input for Penetrating Boxes

```
//  EXEC  MATRIX,REG=500K,OUT=A,ID=3
//*4567890123456789012345678901234567890123456789012345678901234567890123456789012
//MATRIX.CARDS DD *,DCB=BLKSIZE=800
S ISEE-3                      999:00:00:00
SI          78/11/23 00:00:00 79/02/16 00:00:00
SE          78/12/10 00:00:00 78/12/16 00:00:00
SE          78/12/30 00:00:00 79/01/01 00:00:00
SE          79/01/21 00:00:00 79/01/23 00:00:00
P B1      C1               FFFFF1FFFFFFFFF                  01 00010001      X
       ff
P B1      C1               FFFFF1FFFFFFFFF                  01 00020002      X
       ff
P B1      C1               FFFFF1FFFFFFFFF                  01 00030003      X
       ff
P B1      C1               FFFFF1FFFFFFFFF                  01 00040004      X
       ff
P B1      C1               FFFFF1FFFFFFFFF                  01 00050005      X
       ff
P B1      C1               FFFFF1FFFFFFFFF                  01 00060006      X
       ff
P B1      C1               FFFFF1FFFFFFFFF                  01 00070007      X
       ff
P B1      C1               FFFFF1FFFFFFFFF                  01 00080008      X
       ff
P B1      C1               FFFFF1FFFFFFFFF                  01 00090009      X
       ff
P B1      C1               FFFFF1FFFFFFFFF                  01 00100010      X
       ff
P B1      C1               FFFFF1FFFFFFFFF                  01 00110011      X
       ff
P B1      C1               FFFFF1FFFFFFFFF                  01 00120012      X
       ff
P B1      C1               FFFFF1FFFFFFFFF                  01 00130013
       ff
P B1      C1               FFFFF1FFFFFFFFF                  01 00140014      X
       ff
P B1      C1               FFFFF1FFFFFFFFF                  01 00150015      X
       ff
P B1      C1               FFFFF1FFFFFFFFF                  01 00160016      X
       ff
P B1      C1               FFFFF1FFFFFFFFF                  01 00170017      X
       ff
P B1      C1               FFFFF1FFFFFFFFF                  01 00180018      X
       ff
P B1      C1               FFFFF1FFFFFFFFF                  01 00190019      X
       ff
P B1      C1               FFFFF1FFFFFFFFF                  01 00200020      X
       ff
P B1      C1               FFFFF1FFFFFFFFF                  01 00210021      X
       ff
P B1      C1               FFFFF1FFFFFFFFF                  01 00220022      X
       ff
P B1      C1               FFFFF1FFFFFFFFF                  01 00230023      X
       ff
P B1      C1               FFFFF1FFFFFFFFF                  01 00240024      X
       ff
P B1      C1               FFFFF1FFFFFFFFF                  01 00250025      X
       ff
```

SECTION 3 - GENERATION OF RESPONSE MODES

This step in the calibration uses existing computer programs that incorporate range/energy theory and geometry factor calculation to assign energies and geometries to the delineated tracks from the program plots. This information is used to create tables called response modes.

Briefly, the following steps are performed:

1. Find the endpoint energy for each mass line. The initial detector description is edited and used in a specified manner with the range/energy program TESTM to yield the endpoint energies.
2. Use the endpoint channel values determined earlier in the calibration process to
   a. calculate the energy per channel and
   b. calculate the Full Scale MeV.
3. Edit, as needed, the detector description, resetting the FSMeV and channel offset values in the description.
4. Run the range/energy program TESTM with the detector description from above. This program generates the energy deposited in each detector, in channel units, from the range of initial particle energies. (See Section 3.1 of this volume and Appendix G of Volume I for discussions of the response generation programs.)
5. Run the program BXGNEW which generates a model track with associated energies and geometry factors for a given particle, gain, and data type. If the box-spread and overlap priority options (see Appendix B below) are used to form an actual TRACK that TRACK should overlay the data TRACK very well.

Figure 1 illustrates the computer generated track from the program BOXGEN for the 881 1 proton particle mode TAB. Figure 2 shows the data to which the track should be compared.

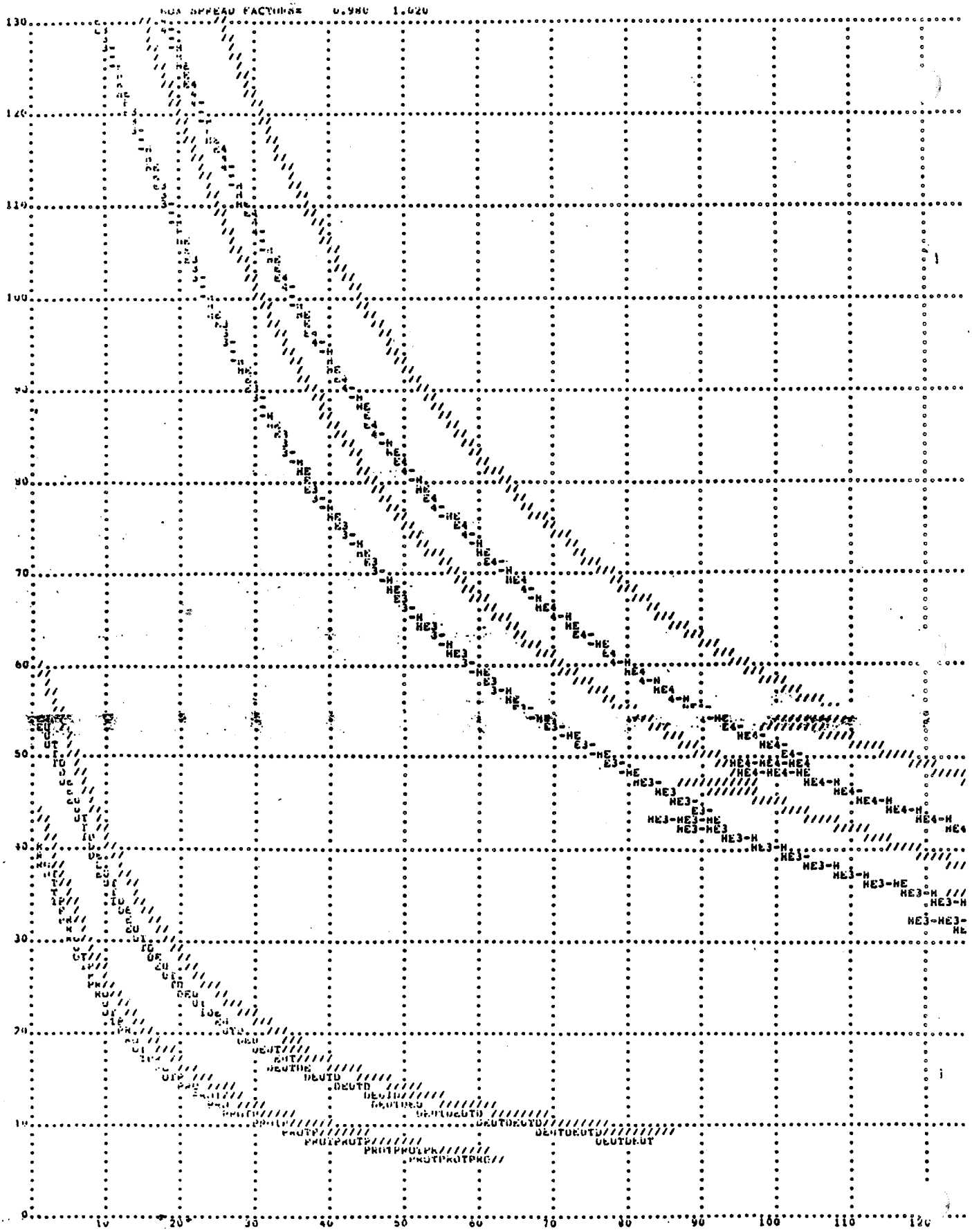

Figure 1. Computer Generated Track for Mode IA3

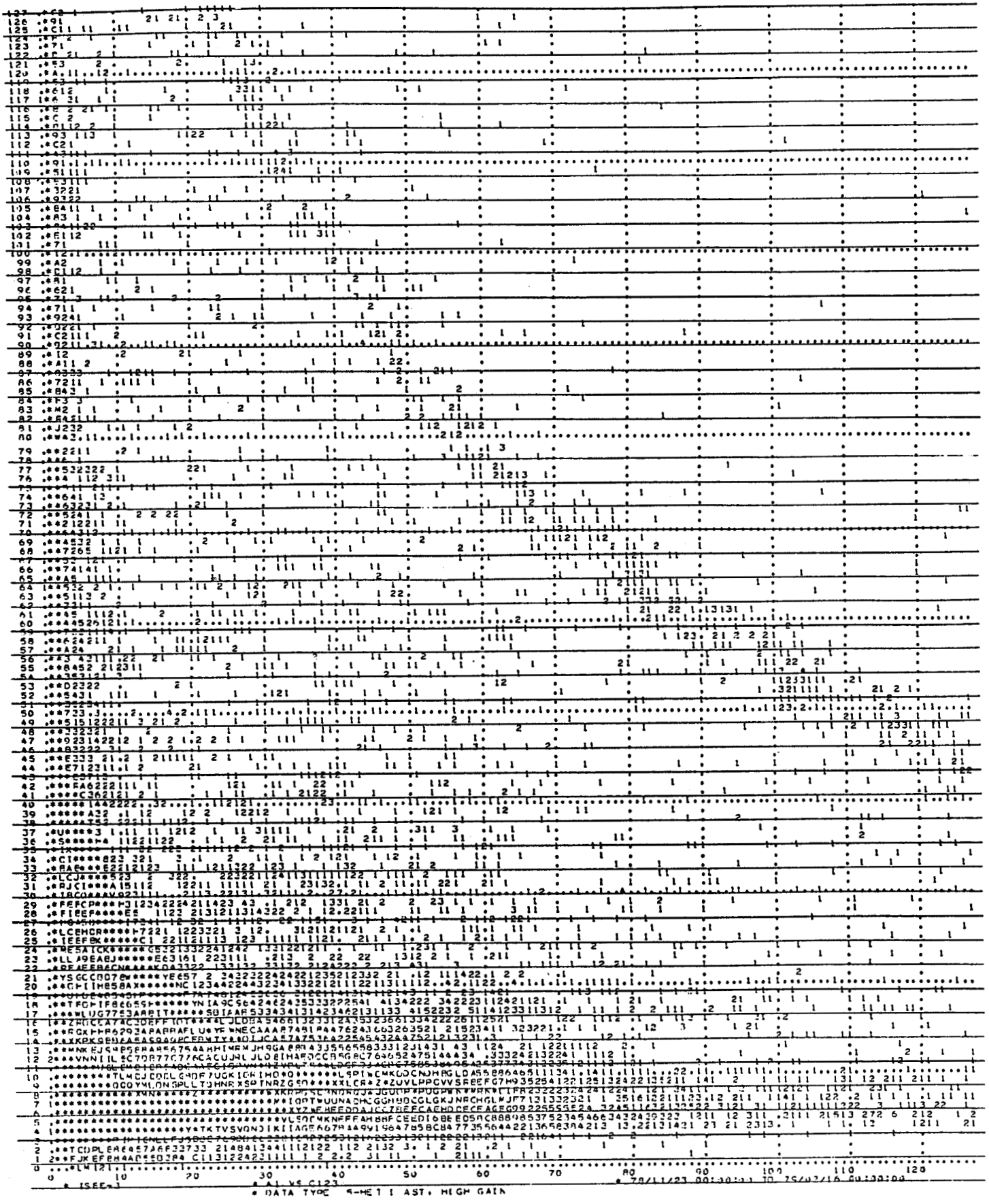

Figure 2. Data for Mode IA3

For ISEE-3, the computer tracks were not used for penetrating modes, so the generated track is hand edited to contain the GATRAX program delineated track. Appendix C contains one example of a hand delineated track. The edited tracks are subdivided into "response mode" regions. These are specific energy regions along the track which are considered separately in the further data analysis. These energy regions are requested by the scientist using the data.

6. Enter the response modes in the calibration dataset SB#IC.CATALOG.DATA. The dead layer energy assignments are made during this calibration step. The programs TESTA and BOXGEN indicate where dead layers fall in the energy loss process. (see below) These energy regions are simply noted for each response mode.

The geometry factor calculation has been built into TESTM and is automatically output in the track generation. Appendices G and H in Volume I contain more detailed information on the geometry calculation as TESTM and BXGNEW handle it. However, for certain classes of penetrating type events, it is not possible to distinguish whether the event came from the A or B end of the telescope. The effective geometry is then multiplied by two to account for this.

A description of these steps is given in the following subsections.

3.1 TESTM: The 11.2 ISEE3 MODEL

The determination of the energy distribution along each mass line requires a model for the behavior of particles passing through the GGT telescope. This model can be modified to represent an average of what the different

particles "see" as the detector. The basic model is built into the program TESTA (see Appendix G of Volume 1).

The initial detector model in TESTA describes the HETs as designed using a perpendicular entry into the telescope for particles and a maximal angle of entry. However, a detector model, which has been modified to simulate an average angle of entry into the stack at 11.2 degrees, has been used to generate the penetrating RESPONSE mode tables for ISEE-3. This angle represents the path of mean entry into the detectors. The program TESTM is hardcoded to calculate an 11.2 degree angle of entry into the HETs. It differs from TESTA in that respect only; the maximal angle of entry calculation in TESTM is ignored.

3.1.1 THE DETECTOR DESCRIPTION

Simulation of particle tracks through the detector stack is accomplished with the use of TESTM and a detector description file. The detector description file contains detector and dead layer thicknesses, detector spacings, offsets, PSMeV, the type of particles, and the gains that can currently be analyzed. The Flight 2 telescope thickness specifications are given in Table 5. The ISEE-3 detector descriptions for HET I are given in Table 6 and HET II in Table 7.

The HET detectors onboard ISEE-3 consist of eleven elements (A1, A2, B1, B2, C1, C2, C3, C4) (see Figure 3), and operate with high or low gain in four possible modes (A stopping, B stopping, A penetrating, and B penetrating). These terms are discussed in detail in Appendix A of Volume 1.

The structure of Tables 6 and 7 is identical. The first column lists the element; blanks in this column refer to a

Table 5. ISEE-3 SRD Dead Layer Thicknesses

ISEE-C HET TELESCOPE DATA

HET 1 (T-7)

DETECTOR ELEMENT	DETECTOR TYPE	SERIAL NUMBER	NOMINAL (μm)	MEASURED SENSITIVE THICKNESS (μm) CENTER	TOP	BOTTOM	LEFT	RIGHT	DEADLAYER (μm)
A1	SB	16-758C	150	148.1	150.2	148	148	146.4	119.2μgm/cm^{2}Aℓ
A2	SB	17-648E	150	150.8	151.8	152.2	149.9	149.5	120 "
C1	LD	2273	3000						81
$C2_A$	LD	2286	3000						74
$C2_B$	LD	2292	3000						97
$C3_A$	LD	2489	3000						61
$C3_B$	LD	2453	3000						82
$C4_A$	LD	2352	3000						74
$C4_B$	LD	2293	3000						66
B1	LD	2361	2000						68
B2	LD	2200	2000						84

HET 2 (T-8)

A1	SB	16-758E	150	149.5	148.3	151.5	148.4	147.7	119.2μgm/cm^{2}Aℓ
A2	SB	16-390A	150	155.1	152.4	153.2	150.7	154.4	120 "
C1	LD	2277	3000						84
$C2_A$	LD	2291	3000						70
$C2_B$	LD	2263	3000						101
$C3_A$	LD	2287	3000						70
$C3_B$	LD	2271	3000						72
$C4_A$	LD	2268	3000						77
$C4_B$	LD	2043	3000						71
B1	LD	2126	2000						74
B2	LD	2137	2000						61

FOILS: A END = 0.0005" CAPTON
B END = 0.001" CAPTON

DETECTOR AREA SPECIFICATIONS
A - 800mm^2; +40mm^2, -0
B - 800mm^2; +40mm^2, -0
C - 900mm^2; +45mm^2, -0

DETECTOR DEPTH SPECIFICATIONS
A - 150μm; ±7.5μm
B - 2000μm; +100μm, -0
C - 3000μm; +150μm, -0

Table 6. HET I Detector Description for all Penetrating Modes

```
C  I  ISEE  HET1  CALIB (ENTERED 2/9/81)  MODIFIED FROM [200,105]TH1L0Z.DET
C       PEN OFFSETS SET TO 2.3; FMOD PEN FSMEV  C3 THICK NE, SPAC,RADIUS AS VOYAGER
C       FILE NAME: ICTC3.DET
C
C     MODES      GAINS
C        4           2
C
C
C ELEM    NO. THICK AMP-AST  BST    PEN THRESHOLDS SPACING  RADIUS CURV
C           0    16       7    7      7                  0   15960    1
C     A1    1   148       1    7      7     -.63    -.13  68314   15960    1
C     A2    2   151       2    7      7     -.62    -.12   2592   15960    1
C     C1    3  2920       3    6      2      2.5      .5      0   17131    1
C           0    81       7    7      7                      1851   17131    1
C     C2    4  2925       4    5      5     4.68     .92    671   17131    1
C           0   171       7    7      7                      672   17131    1
C     C2    4  2900       4    5      5     4.68     .92   1851   17131    1
C     C3    5  2939       5    4      4     4.66     .92    671   17131    1
C           0   143       7    7      7                      672   17131    1
C     C3    5  2918       5    4      4     4.66     .92   1851   17131    1
C     C4    6  2925       6    3      3     4.69     .92    671   17131    1
C           0   140       7    7      7                      672   17131    1
C     C4    6  2935       6    3      3     4.69     .92   2473   17131    1
C           0    68       7    7      7                      0   15960    2
C     B2    7  1930  2150  7    2      7     2.13     .3  53607   15960    2
C     B1    8 -1915  2306  7    1      1     1.09     .3      0   15960    3
C           0    84       7    7      7                      0   15960    3
C           0    33       7    7      7                      0   15960    1
C
C              LOW GAIN                    HIGH GAIN
CHANNELS     OFFSET      FSMEV       OFFSET      FSMEV
    4096       1.60        953.        0.          200.    .0483   AST   A1
    4096       -.51        931.        0.          197.4   .0483   AST   A2
    4096        .94      17833.         .5         3533.   .1802   AST   C1
    4096        .33      17992.        0.          3603.   .1802   AST   C2
    4096        .12      17999.        0.          3680.   .1833   AST   C3
    4096       1.35       2494.       1.5          747.    .1833   PEN & BST B1
    4096        .64       4910.        1.          755.            BST   B2
    4096       0.00      17490.      0.00         3617.            PEN & BST C4
    4096        .00      17490.        0.         3617.            PEN & BST C3
    4096       2.30      17490.       2.3         3617.    .1831   PEN & BST C2
    4096       1.19       5143.      1.76         1016.            PEN   C1
C
C                        SLANT 1                     SLANT 2
C   1     2 BOTH  GN    CH1    CH2    CH3    SUM    CH1    CH2    CH3    SUM
  SA1   SA2    SA    1     1.      .6   .375   -39.     1.      .6   5.43  -105.
        SB     SB    2                               1.     1.     1.    -60.
        SB     SB    2                               1.     1.     1.    -60.
C
C            NUMBER OF SPECIES
C     MODES  LO GAIN    HI GAIN
C        4           1           2
C
C  LOW GAIN:
C NAME      Z          A
C HE3-      2     3.0149
  HE4-      2     4.0015
C LI6-      3       6.00
C BE9-      4       9.00
C B11-      5      11.00
C C12-      6      12.00
C N14-      7      14.00
C O16-      8      15.99
C F19-      9      18.99
C NE20     10      19.99
C NA23     11      22.99
C MG24     12      23.99
C
C  HIGH GAIN:
  PROT      1     1.0073
C DEUT      1     2.0136
C HE3-      2     3.0149
  HE4-      2     4.0015
```

Table 7. HET II Detector Description for all Penetrating Modes

```
IT TSEE  HET2  CALIB (ENTERED 2/9/81) MODIFIED FROM [200,105]TH2L0Z.DET
C    PEN OFFSET = 2.3: FMOD PEN FSMEV   SPAC,RADIUS AS IN VOYAGER
C       FILE NAME: ICITG3.DET
C
C     MODES      GAINS
C       4          2
C
C
C ELEM    NO.  THICK  AMP-AST   BST    PEN  THRESHOLDS  SPACING   RADIUS  CURV
C            0     16       7     7      7                     0    15960     1
C     A1     1    149       1     7      7    -.63    -.13  68313    15960     1
C     A2     2    153       2     7      7    -.62    -.12   2590    15960     1
C     C1     3   2915       3     6      2   2.49     .75      0    17131     1
C            0     84       7     7      7                  1851    17131     1
C     C2     4   2930       4     5      5   4.65     .92    671    17131     1
C            0    171       7     7      7                   672    17131     1
C     C2     4   2900       4     5      5   4.65     .92   1851    17131     1
C     C3     5   2930       5     4      4   4.68     .92    671    17131     1
C            0    142       7     7      7                   672    17131     1
C     C3     5   2930       5     4      4   4.68     .92   1851    17131     1
C     C4     6   2920       6     3      3   4.69     .92    671    17131     1
C            0    148       7     7      7                   672    17131     1
C     C4     6   2930       6     3      3   4.69     .92   2743    17131     1
C            0     74       7     7      7                     0    15960     2
C     B2     7   1925 2205  7     2      7   2.04     .3   53607    15960     2
C     B1     8   1925 2125  7     1      1   1.00     .3       0    15960     3
C            0     61       7     7      7                     0    15960     3
C            0     33       7     7      7                     0    15960     1
C
C                 LOW GAIN                HIGH GAIN
CHANNELS      OFFSET      FSMEV       OFFSET      FSMEV
   4096         1.70       958.         .60       202.1      AST A1
   4096         -.27       938.        -.20       195.6      AST A2
   4096          .94     18128.          .2      3687.      AST C1
   4096         -.04     18243.          .08     3712.      AST C2
   4096          .13     17630.          .30     3548.      AST C3
   4096         1.68      2542.         1.00      785.      PEN & BST B1
   4096         1.07      4998.          .96      800.      BST B2
   4096         0.00     17203.         0.00     3658.      PEN & BST C4
   4096         0.00     17203.          .00     3658.      PEN & BST C3
   4096         2.30     17203.         2.30     3658.      PEN & BST C2
   4096         1.09      5150.         1.43     1053.      PEN C1
C
C
C                          SLANT 1                    SLANT 2
C   1    2 BOTH   GN    CH1    CH2    CH3    SUM    CH1    CH2    CH3    SUM
  SA1  SA2   SA    1     1.      .6   .375   -39.     1.      .6   5.43  -105.
       SB    SB    2                                 1.     1.     1.    -60.
       SB    SB    2                                 1.     1.     1.    -60.
C
C            NUMBER OF SPECIES
C     MODES  LO GAIN    HI GAIN
C       3 (4)     01          2
C
C  LOW GAIN:
C NAME      Z          A
C HE3-      2     3.0149
C HE4-      2     4.0015
C LI7-      3       7.00
C BE9-      4       9.00
C B11-      5      11.00
C C12-      6      12.00
C N14-      7      14.00
C O16-      8      15.99
C F19-      9      18.99
C NE20     10      19.99
C NA23     11      22.99
C MG24     12      23.99
C
C  HIGH GAIN:
   PROT     1     1.0073
C DEUT      1     2.0136
C HE3-      2     3.0149
   HE4-     2     4.0015
```

dead layer. Note that C2, C3, C4 each consist of two elements. Column 2 lists the element number starting with the A end of the telescope. Dead layers are denoted by 0. Column 3 gives the thickness of the layer in micrometers. Columns 4, 5, 6 list the values of the flag for the logic equation to denote A stopping, B stopping, and penetrating events, respectively. Columns 7 and 8 give the minimum energy (in MeV) needed to penetrate that layer for low and high gain, respectively. The distance (in micrometers) to the next layer is given in column 9. Detector measurements are given as spacings between elements. There are two conventions

1. For A-side spacings, the draftsman convention is to measure in inches from the top of the A1 detector to the top of each remaining detector layer .
2. For B-side spacings, the measurement is made from the bottom of the B1 detector to the bottom of each detector layer. Other reference measurements are available on the B end, one of which was used in the spacings derivation.

The derivation of HET spacings used in the detector description files is shown in Figure 4. Distances are taken from the draftsman HET telescope diagram dated March 16, 1981. This HET is typical of all Voyager and ISEE-3 HET telescopes.

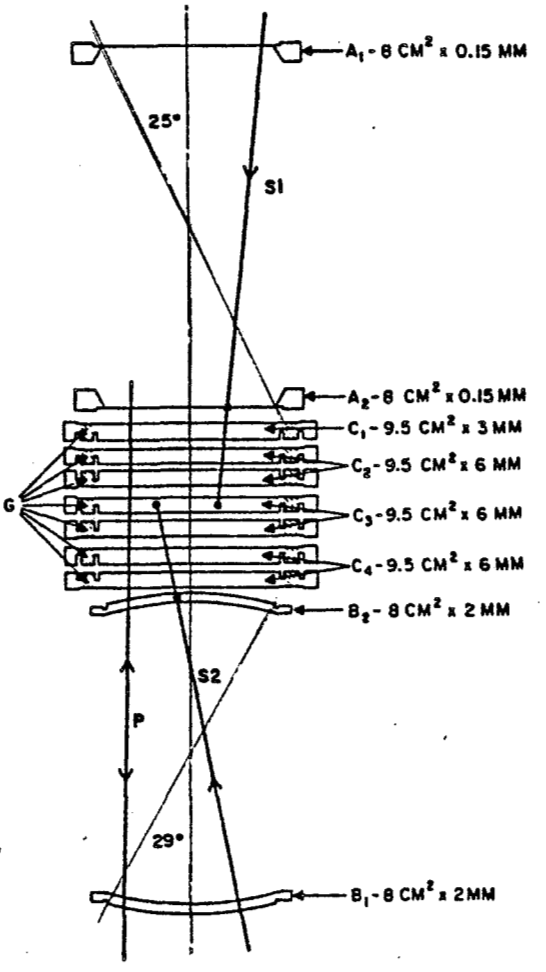

Figure 3. HET Detector Schematic Diagram

A schematic cross-sectional view of a HET telescope on ISEE-3 and Voyagers 1 and 2. Trajectories 1, 2, and 3 correspond to three different event types identified by the coincidental/anticoincidental logic.

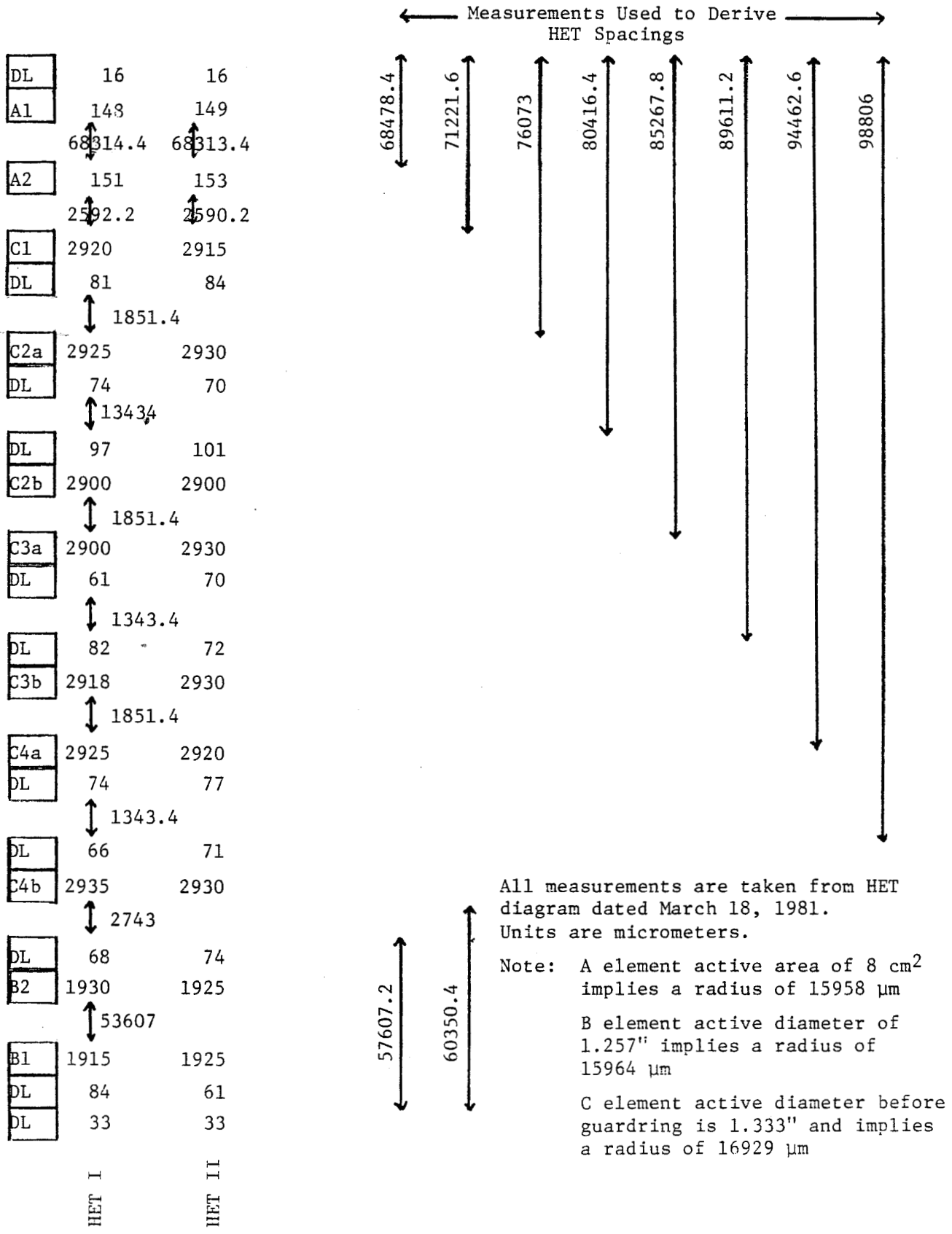

Figure 4. HET Spacing Derivation

The detector description used for calculations uses spacings between layers in micrometers. The radius (in micrometers) of the layer is given in column 10. Column 11 denotes the curvature of the layer. All layers are flat (CURV=1) with the exception of the E detectors (CURV = 2 or CURV=3, first surface convex or concave as seen from the A end of the HET).

The next part of the table lists information regarding the energy that can be measured with each detector. The first column gives the number of units, or channels, available in which pulse data can be stored. All detectors have the same number of channels, 4096. Each detector, however, has its own upper energy limit that it can measure. This maximum detectable energy is called the Full Scale MeV value. These are given in columns 3 and 5. The offsets in columns 2 and 4 represent zero points, i.e., energy values when no energy has been deposited in the detector. The offsets are given for both low and high gain. Gain effectively serves as a scale factor which changes the maximum energy presented as input to the analog-to-digital converter. The last column lists the mode and the detector. The ampersand (&) indicates that the entry is used for penetrating and B stopping events.

The third part of the table lists the coefficients and the sum to be used to determine slant threshold. These thresholds, discussed in Appendix A of Volume I, are electronic summing techniques to eliminate some range of events or background counts.

The last section lists types of particles being analyzed along with their atomic number and atomic weight. These data along with all other data in the table serve as input to the TESTM program.

These detector description files are located in datasets on the PDP 11/70. The file names for the penetrating modes are [200,106]ICHETI.DET and [200,106]ICHETII.DET. and are shown above in Tables 6 and 7.

The two- and three-dimensional stopping mode detector description files which were used in the Reames work are shown in Appendix B with the TESTA/ECXGEN documentation.

3.2 DETERMINATION OF ENERGY/CHANNEL AND FSMEV

To determine the FSMeV, it is necessary to know the energy that corresponds to the point of penetration through the detector for a given particle species. The program IESTM generates the energy deposited in each detector, in channel units, given an initial energy.

The detector description can change the channel units output of TESTM to energy units output by equating the energy per channel to 1.0. Since

$$FSMeV = E/channel * 4096$$

for all ISEE-3 cases, all FSMeV in the detector description are then equal to 4096. Next, IESTM is run and the detector penetration point is located from the job printout. The detector descriptions used for the ISEE-3 HETs, along with the IESTM output are given in Appendix D. Appendix C of Volume I gives a guide for use of the PDP 11/70 programs. The energy of penetration is not located precisely if a dead layer is present on the exiting side of the detector. A first estimate is made and, along with the estimated channel endpoint location, the energy per channel is calculated:

E/channel = energy of detector penetration/channel of endpoint

Then

$$FSMeV = 4096 * energy/channel$$

Recall that Section 2.1 lists matrix program requests while Appendix A shows graphical endpoint determinations for the C detector stopping example. Appendix B contains information for the A and B detector references. See Appendix D for an example of how to derive the FSmeV energy using TESTM.

3.2.1 DEAD LAYER ENERGIES

The procedures used to determine the HET dead layer regions are described below.

The original thickness and spacings detector description files given in Table 6 for HET I and Table 7 for HET II were used as input to TESTA. The energy increment for varying incident particle energy was 2 percent and all other TESTA default values were used. Under these circumstances the output of TESTA contains TRACK data for the perpendicular entry particle and the maximum angle entry particle. BOXGEN or BXGNEW (see Section 3.3) is then run on that TRACK output for the stopping particle mode. BOXGEN and BXGNEW are equivalent for stopping modes. All BOXGEN defaults were used with box spread factors set to one. BOXGEN indicates with stars the reference detector channel numbers which include dead layers.

The energy range selected for the dead layer would start with the perpendicular track energy of the first starred channel number. The range would end with the maximally inclined energy of the last starred channel number.

The basic dead layer regions have been rounded to integer values and are summarized below in Section 4. Appendix E lists BOXGEN output with the dead layer selection illustrated. The bracket indicates the limits selected in each case.

BOXGEN output gives the lowest energy for the transition

(n - 1) ----> n

for stopping modes in the perpendicular entry data TRACK. It gives the largest possible energy occurring in that channel in the maximally inclined data TRACK. The location of the dead layers relative to the detector faces is shown in Figure 4 .

3.3 GENERATING RESPONSE MODES

Once parameter values for FSHeV and CFFSETS have been decided upon for the current calibration iteration, response mode table generation can be done.

The necessary steps in this process are described below. Programs that are referenced are listed with their locations in Appendix B of Volume 1. The location of the programs TESTM and BXGNEW is given in Appendix F of Volume 2 of the Document. Use of the programs is demonstrated in Appendix C of Volume 1.

First, the existing description detector datasets on the PDP 11/70 are edited to change any detector parameters for which modifications are desired (e.g., detector offsets, FSHeV, thickness, etc.).

Then, the program TESTM is executed. TESTM produces a table of range versus energy through the detector stack for various particles and incident energies. The detector description referenced above serves as input to TESTM . A PDP 11/70 dataset is the output. A 2 percent energy increment is selected to yield the desired 2 percent accuracy (as illustrated in Appendix C of Volume 1). TESTM automatically outputs the geometry factors into the PDP 11/70 dataset.

Next, the program BXGNEW is executed. The IESTM output dataset along with information about the particle, gain, and mode (penetrating or two- or three-dimensional stopping region of the track) serves as input for each case required. This creates a PDP 11/70 output dataset that is subsequently edited by the user. BXGNEW assigns channel values along the track for all detectors involved in a particular user request. It also associates an energy with each "reference detector channel number." (For stopping modes, the reference detector is the detector in which the particle stopped. For penetrating modes, the reference detector is the sum C stack.) The tracks generated by BXGNEW for penetrating modes have not been used in the actual tables; rather, the track definitions have been supplied by GSFC scientists.

The BXGNEW output file is then edited for mode name, mode start and stop reference detector channel limits and, if necessary, geometry factor. Note that the geometry factor must be doubled for bi-directional modes. If installing or re-installing (see Section 3.4), the track definitions must be edited. In the editing, no lines may be added to or deleted from the existing BXGNEW output dataset (see Appendix C of Volume I).

Next, BXGNEW is re-executed. During this execution the tape-write option is enabled (and the create output file option is disabled). BXGNEW takes the edited response file, writes it to tape with one tape file generated for each response. This tape serves as input to the INSTALL and OVRLAY programs (See Section 3.4).

Table 8 shows the BXGNEW requests to generate some representative modes. Table 9 shows a typical BXGNEW output file with editing notes. The subsequent tape generation step is shown in Table 10.

Table 8 Typical BXGNEW TRACK Request

particle catalog name	mode-name mnemonic	BXGNEW Track Request
HE4	IA2	A-stopping, 2-dimensional, high gain HET-1
	IA3	A-stopping, 3-dimensional, high gain HET-1
	IB2	B-stopping, 2-dimensional, high gain HET-1
	IL3	B-stopping, 3-dimensional, low gain HET-1
PROTON	IA2	A-stopping, 2-dimensional, high gain HET-1
	IA3	A-stopping, 3-dimensional, high gain HET-1
	IB3	B-stopping, 3-dimensional, high gain HET-1
ALPHA	IPH	B-penetrating, 3-dimensional, high gain HET-1
	IPZ	A-penetrating, 3-dimensional, high gain HET-1
	IPY	B-penetrating, 3-dimensional, high gain HET-1
	IIP	B-penetrating, 3-dimensional, low gain HET-2
	IIPA	A-penetrating, 3-dimensional, low gain HET-2
	IIPB	B-penetrating, 3-dimensional, low gain HET-2

note For 2-dimensional STOPPING modes in VOYAGER, request a 1 or 0 dimension. BXGNEW defaults to the 'sum of channel' reference technique which is used by the ISEE 2-dimensional modes.

Normally, BXGNEW is run accepting all defaults and specifying box spread factors of 1 for penetrating modes.

Table 9.   BXGNEW Output File with Editing Notes

```
FILE   1 -          57 RECORDS IN    1 BLOCKS        13-SEP-82
C    I  ISEE  HET1  CALIB (ENTERED 2/9/81)  MODIFIED FROM REOR,1
C    DETECTOR FILE ICIG3.DET              ,TRACK FILE ICIG3.TRK
C    B-PENETRATING                    LOW GAIN
C
C      P-                             28
* IL3L   HE4-          2       4.002       (57)        70.656   2400.201
      3          50      1          8               6          24          3        73       268
```

9	8**	6	6	4	4	2400.201	2400.201	0.4219
10	9**	6	7	4	5	1695.277	1695.277	0.8438
11	10**	7	7	5	6	737.086	737.086	0.8438
12	11**	7	8	6	6	519.556	519.556	0.8438
13	12**	8	9	6	7	405.438	405.438	0.8438
14	13**	9	10	7	7	334.077	334.077	0.8439
15	14**	10	10	7	8	286.041	286.041	0.8438
16	15**	10	11	8	9	251.078	251.078	0.8438
17	16**	11	12	9	9	223.629	223.629	0.8438
18	17**	12	12	9	10	200.598	200.598	0.8438
19	18**	12	13	10	11	183.236	183.236	0.8438
20	19**	13	14	11	11	168.807	168.807	0.8438
21	20**	14	14	11	12	156.951	156.951	0.8438
22	21**	14	15	12	13	146.924	146.924	0.8438
23	22**	15	15	13	14	138.223	138.223	0.8438
24	23**	15	16	14	14	130.470	130.470	0.8438
25	24**	16	16	14	15	124.178	124.178	0.8438
26	25**	16	17	15	16	118.265	118.265	0.8439
27	26**	17	17	16	17	113.235	113.235	0.8438
28	27**	17	18	17	18	108.778	108.778	0.8438
29	28**	18	18	18	19	104.801	104.801	0.8438
30	29**	18	19	19	20	101.236	101.236	0.8438
31	30**	19	19	20	21	98.137	98.137	0.8438
32	31**	19	20	21	22	95.251	95.251	0.8438
33	32**	20	20	22	24	92.685	92.685	0.8438
34	33**	20	20	24	25	90.395	90.395	0.8438
35	34**	20	21	25	27	88.321	88.321	0.8438
36	35**	21	21	27	29	86.439	86.439	0.8438
37	36**	21	21	29	30	84.729	84.729	0.8438
38	37**	21	21	30	33	83.177	83.177	0.8438
39	38**	21	22	33	35	81.790	81.790	0.8438
40	39**	22	22	35	38	80.524	80.524	0.8438
41	40**	22	22	38	42	79.337	79.337	0.8438
42	41**	22	22	42	47	78.285	78.285	0.8438
43	42**	22	23	47	55	77.331	77.331	0.8438
44	43**	23	23	55	73	76.467	76.467	0.8447
45	44**	23	23	67	73	75.682	75.682	0.8506
46	45**	23	23	61	67	74.974	74.974	0.8574
47	46**	23	23	55	61	74.335	74.335	0.8640
48	47**	23	23	50	55	73.759	73.759	0.8686
49	48**	23	23	45	50	73.243	73.243	0.8746
50	49**	23	24	40	45	72.779	72.779	0.8785
51	50**	24	24	35	40	72.371	72.371	0.8824
52	51**	24	24	30	35	72.010	72.010	0.8860
53	52**	24	24	25	30	71.691	71.691	0.8876
54	53**	24	24	20	25	71.416	71.416	0.8905
55	54**	24	24	16	20	71.189	71.189	0.8935
56	55**	24	24	10	16	70.986	70.986	0.8944
57	56**	24	24	4	10	70.841	70.841	0.8960
58	57**	24	24	3	4	70.696	70.696	0.8969

geom = 1.6876

Table 10.   BXGNEW Output for Tape

```
FILE   1 -        57 RECORDS IN    1 BLOCKS       13-SEP-82
C    I  ISEE   HET1  CALIB (ENTERED 2/9/81)  MODIFIED FROM REOR,1
C    DETECTOR FILE ICIG3.DET              ,TRACK FILE ICIG3.TRK
C    B-PENETRATING                      LOW GAIN
C
C
* IP L    HE4-              2       4.002             70.656   2400.201
       3            50         1        8       28          6        24         3        73          268
```

9	8**	6	6	4	4	2400.201	2400.201	1.6876
10	9**	6	7	4	5	1695.277	1695.277	1.6876
11	10**	7	7	5	6	737.086	737.086	1.6876
12	11**	7	8	6	6	519.556	519.556	1.6876
13	12**	8	9	6	7	405.438	405.438	1.6876
14	13**	9	10	7	7	334.077	334.077	1.6876
15	14**	10	10	7	8	286.041	286.041	1.6876
16	15**	10	11	8	9	251.078	251.078	1.6876
17	16**	11	12	9	9	223.629	223.629	1.6876
18	17**	12	12	9	10	200.598	200.598	1.6876
19	18**	12	13	10	11	183.236	183.236	1.6876
20	19**	13	14	11	11	168.807	168.807	1.6876
21	20**	14	14	11	12	156.951	156.951	1.6876
22	21**	14	15	12	13	146.924	146.924	1.6876
23	22**	15	15	13	14	138.223	138.223	1.6876
24	23**	15	16	14	14	130.470	130.470	1.6876
25	24**	16	16	14	15	124.178	124.178	1.6876
26	25**	16	17	15	16	118.265	118.265	1.6876
27	26**	17	17	16	17	113.235	113.235	1.6876
28	27**	17	18	17	18	108.778	108.778	1.6876
29	28**	18	18	18	19	104.801	104.801	1.6876
30	29**	18	19	19	20	101.236	101.236	1.6876
31	30**	19	19	20	21	98.137	98.137	1.6876
32	31**	19	20	21	22	95.251	95.251	0.8438
33	32**	20	20	22	24	92.685	92.685	0.8438
34	33**	20	20	24	25	90.395	90.395	0.8438
35	34**	20	21	25	27	88.321	88.321	0.8438
36	35**	21	21	27	29	86.439	86.439	0.8438
37	36**	21	21	29	30	84.729	84.729	0.8438
38	37**	21	21	30	33	83.177	83.177	0.8438
39	38**	21	22	33	35	81.790	81.790	0.8438
40	39**	22	22	35	38	80.524	80.524	0.8438
41	40**	22	22	38	42	79.337	79.337	0.8438
42	41**	22	22	42	47	78.285	78.285	0.8438
43	42**	22	23	47	55	77.331	77.331	0.8438
44	43**	23	23	55	73	76.467	76.467	0.8442
45	44**	23	23	67	73	75.682	75.682	0.8506
46	45**	23	23	61	67	74.974	74.974	0.8574
47	46**	23	23	55	61	74.335	74.335	0.8640
48	47**	23	23	50	55	73.759	73.759	0.8686
49	48**	23	23	45	50	73.243	73.243	0.8746
50	49**	23	24	40	45	72.779	72.779	0.8786
51	50**	24	24	35	40	72.371	72.371	0.8824
52	51**	24	24	30	35	72.010	72.010	0.8860
53	52**	24	24	25	30	71.691	71.691	0.8876
54	53**	24	24	20	25	71.416	71.416	0.8905
55	54**	24	24	16	20	71.189	71.189	0.8935
56	55**	24	24	10	16	70.986	70.986	0.8944
57	56**	24	24	4	10	70.841	70.841	0.8960
58	57**	24	24	3	4	70.696	70.696	0.8969

Table 11 lists existing ISEE-3 penetrating response modes, with the editing required from the first execution of BXGNEW (i.e., without the tape-write option).

If more than one response mode table is defined along one particle track, BXGNEW is executed once for each mode in exactly the same way. The channel limits would then determine what part of the track is associated with the file's mode name. For example, from the data in Table 9, the mode IP for particle ALPHA is formed. It is associated with the sum C channel limits 8 to 28. The lower energy region is also put into another mode table, the IPB table, which is sum C channels 29 to 38. Two separate sets of data are required, however, differing only in their channel limits (and, in this case, geometry factors).

TESTA /BOXGEN were used (see Appendix B) to generate response modes for two- and three-dimensional stopping particles. The ISACK definitions in those CATALOG.DATA modes were generated from program BOXGEN.

Table 11 Editing Required for BXGNEW Penetrating Mode Output Files

Note: To produce the table

1.) TESIM is run with a 2% energy increment and all other defaults

2.) BXGNEW is run with all defaults and box spread factors of 1.

3.) detector models [200,106]ICHETI.DET and [200,106]ICHETII.DET are used for uni- and bi-directional penetrating modes (see Tables 6 and 7)

4.) only editing for HEI I is given, since only those responses are considered valid at the time of this writing;

5.) no A-side responses are considered useful at this time, and these numbers are also omitted.

Particle	mode	BOXGEN mode name	Edited mode name	Channel limits BOXGEN	Edited limits	Geometry doubled
Alpha	IP	_IL3L	_IP_L	8 57	8 28	yes 1.6876
	IPB	_IL3L	_IPBL	8 57	29 38	no
	IPH	_IB3H	_IPHH	34 268	34 102	yes 1.6876
	IPY	_IB3H	_IPYH	34 268	103 138	no
Proton	IPH	_IB3H	_IPHH	10 68	10 28	yes 1.6876
	IPY	_IB3H	_IPYH	10 68	42 50	no

3.4 INSTALLATION OF THE RESPONSE MODES INTO THE CALIBRATION DATASET

Once the response matrices have been generated by BXGNEW, they may be installed, re-installed, or overlayed. These terms mean the following:

term	meaning
Install	enter a new response mode into the CATALOG.DATA dataset. To accomplish this, the program INSTALC is executed.
Re-install	if the track channel definitions need to be changed, the entire install process must be redone.
Overlay	if the track channel definition is satisfactory, but new energies and geometry factors are being tested, the program OVRLAY is executed.

The BXGNEW generated data are included in the CATALOG.DATA dataset by the programs INSTALC or OVRLAY. Table 12 lists the ISEE-3 data types and their associated mode name mnemonics which are currently defined by INSTALC. This table needs to be updated as other mnemonic names are added. Particle mode names are selected from this list according to the appropriate data type (i.e., event type). Penetrating mode names must have a 'P' after the HET I or II letters because the program FLUXFLCI (see Section 4) expects the P character to refer to a penetrating mode.

When INSTALC is executed, the BXGNEW response mode name must match the appropriate name in Table 12.

When OVRLAY is executed, the BXGNEW response mode name must match one of the existing CATALOG.DATA particle catalog entries for the specific particle being updated. The

Table 12 INSTALC/OVRLAY Mode Names for ISEE-3

	Mode Name Mnemonic	Data Type high gain	low gain
1	IA2	5	6
2	IA3	5	6
3	IB2	7	8
4	IB3	7	8
5	IL2	9	10
6	IL3	9	10
7	IIA2	12	13
8	IIA3	12	13
9	IIB2	14	15
10	IIB3	14	15
11	IIL2	16	16
12	IIL3	16	16
13	ID2	20	20
14	ID3	20	20
15	IID2	22	22
16	IID3	22	22
17	IPA	11	11
18	IPB	11	11
19	IP	11	11
20	IPH	10	10
21	IPZ	10	10
22	IPY	10	10
23	IIPA	18	18
24	IIPB	18	18
25	IIP	18	18
26	IIPH	17	17
27	IIPZ	17	17
28	IIPY	17	17

reference detector channel limits (the second column in Tables 9 and 10) must match or be within the current table limits.

An additional restriction should be noted. The particle catalog in the CATALOG.DATA dataset (which contains a summary listing of the response modes in the main CATALOG for each particle) has space for only 24 response modes for each kind of particle. All overflow entries are classified as ALPHA particles. For ISEE all penetrating modes for alpha particles are classified under particle type ALPHA.

In deciding whether the particle type is ALPHA or He4, both INSTALC and OVRLAY have an input parameter logical flag which the user sets to TRUE or FALSE, depending on the BXGNEW data being used. BXGNEW outputs He4- for all alpha particle responses. If the response being added or changed is the He4 particle type, that parameter should be flagged false. If the response is an ALPHA particle type, that logical parameter should be flagged true.

Sources for the programs and JCL required to execute INSTALC and OVRLAY are located in the dataset SB#IC.LISTHS2.SOURCE in the members:

OVRLAY	OVRLAY program source code
INSTALC	INSTALC program source code
RNOVRLAY	JCL for OVRLAY
INSC	JCL for INSTALC

In practice, the BXGNEW tapes are generated on the Laboratory for High Energy Astrophysics PDP 11/70, while the INSTALC/OVRLAY programs are executed on the SACC IBM 3081. After the tapes are placed in SACC, INSTALC or OVRLAY is executed into a backup copy of the current CATALOG.DATA dataset. Then, the new entries are listed to verify the

backup copy. Next, the current catalog is archived and the backup version is renamed. Finally, it is verified that the backup is in permanent storage and a tape copy has been made.

3.4.1 ALPHA PARTICLE RESPONSE MODE GEOMETRY FACTOR CORRECTION

One other step was done in finalizing the CATALOG.DATA response mode tables. A correction for nuclear interaction processes was applied to the geometry factors of all uni- and bi-directional penetrating alpha mode response tables. These geometry factors were all divided by the factor 1.12 .

The program MODGEOM, which is located in the LISTHS2.SOURCE dataset, was used to accomplish the changes. It is used as a foreground executing CLIST controlled utility in which the user inputs the particle and mode to be updated, and the correction factor. (The program has the capability of changing individual geometry entries, or segments of geometry factors.)

3.4.2 LOCATING AND LISTING INFORMATION ABOUT THE RESPONSE MODES IN THE CATALOG.DATA DATASET

Foreground and background executing capabilities exist for listing response mode entries. They can also be plotted. The dataset SS#IC.LISTHS2.SOURCE contains sources and JCL for those jobs. Background listing and/or plotting JCL on the IBM 3081 computers is in the member RUNIL2V. Foreground listing of response modes on the IBM 3081 computers can be done by executing SS#IC.LIB.CLIST(ALSPONSE). The member USERGIDE contains some information about the listing and plotting options. The reader is again referred to Appendix B in Volume I for a summary of relevant programs.

If it is necessary to change specified words in the CATALOG.DATA dataset, the member FORMATS in SB#IC.LISTHS2.SOURCE is available for help in locating those CATALOG STORAGE words. FORMATS is most easily used in conjunction with a hexadecimal CATALOG DUMP to locate the correct satellite, detector record, particle catalog, and response mode. The listing program above gives the catalog record numbers containing the response modes but not the particle catalog summary entry record and start word. A foreground executing utility called DIRFIX (which lists and changes words of data) can be used, in lieu of a hex dump, to locate data, but this process is very tedious. Extreme care must be exercised if DIRFIX is used and only the cognizant programmer should carry out the changes.

SECTION 4 - EXECUTING THE FLUXPLOT PROGRAM

Once response modes have been put into the CATALOG.DATA dataset, the FLUXPLOT program is used to generate summaries of fluxes within energy subregions of the response mode tables. The resulting fluxes should be compared and checked for self-consistency. For example, A-stopping and B-stopping flux values should agree for regions where particle energies overlap. A second self-consistency criterion is the comparison of the alpha particle tracks for high and low gain settings. The fluxes calculated for overlapping energy regions along these tracks should agree within experimental error. Finally, the HET I and HET II telescopes essentially have the same design. Their flux values are expected to agree to better than 10% neglecting anisotropies in the flux.

4.1 OFFSET DETERMINATION

Offsets are determined for the detectors by demanding flux consistency between the low and high gain alpha particles, between HETs, and with the proton data. Initial offsets for the Sum C detectors are set to zero. Spectral flux plots are made of data which reflect the zero offsets. In an iterative fashion the offset parameter is increased or decreased in such a way as to enhance the above self-consistency.

4.2 FLUX RESULTS

Tables 13 and 14 show data card input for FLUXPLOT and the final output obtained. Plots can be either computer generated or hand drawn from the final output. Energy subregions or BINS within individual response modes are summarized. In selecting these BINS for stopping particle

modes, each dead layer energy range must be completely surrounded by the energy range of the desired BIN which is near it. Figure 5 is a plot of the flux data listed in Table 14 for the penetrating modes indicated in Table 13. Figures 6 through 8 show plots of fluxes for other time periods. Table 15 lists the FLUXPLOT program time input which generated the data plotted in Figures 6 through 8. The data are contained in the book ISEE-3 CALIBRATION: 14.

The JCL to run FLUXPLOT is found in SB#IC.LIB.CNTL(FLUXPLOT). A data deck like that of Table 13 must be appended to the JCL.

A user guide for FLUXPLOT can be found in SB#IC.USERGIDE.TEXT(FLUXPLOT).

Table 13. FLUXPLOT Card Input (1 of 2)

```
S  ISEE-3                       SSS 00 00 00          0.096  IIE  FFT  IFT  1    00000050   0
SI          78 11 23 00 00 00 79 02 16 00 00 00                                  00000060   0
SE          78 12 10 00 00 00 78 12 16 00 00 00                                  00000070   0
SE          78 12 30 00 00 00 79 01 01 00 00 00                                  00000080   0
SE          79 01 10 00 00 00 79 01 10 04 00 00                                  00000085   0
SE          79 01 21 00 00 00 79 01 23 00 00 00                                  00000090   0
SE          79 01 25 00 00 00 79 01 25 12 00 00                                  00000100   0
SE          79 01 31 20 00 00 79 02 01 00 00 00                                  00000110   0
F  FE4                                                                           00000010   0
M  IA2                 Y Y                 1.0E-05   1.0E-03                     00000020   0
B    4.01       5.85          Y                                                  00000030   0
M  IA3                                                                           00000040   0
B    6.210      10.020                                                           00000050   0
B    10.020     16.030                                                           00000060   0
B    16.030     27.160                                                           00000070   0
M  IB2                                                                           00000080   0
B    17.880     26.70                                                            00000090   0
M  MEAN                                                                         X00000100
                                           IE2    IL2                            00000110   0
B    17.880     26.30                                                            00000120   0
M  MEAN                                                                         X00000130
                                           IA3    IB3                            00000140   0
E    27.900     42.10                                                            00000150   0
B    42.100     56.400                                                           00000160   0
M  MEAN                                                                         X00000170
                                           IE3    IL3                            00000180   0
B    27.241     42.000                                                           00000190   0
B    42.000     56.060                                                           00000200   0
B    56.060     65.36                                                            00000210   0
F  ALPHA                                                                         00000220   0
M  IPE                                                                           00000230   0
B     80.520    101.240                                                          00000240   0
M  IPY                                                                           00000250   0
B     96.420    112.118                                                          00000260   0
B    112.118    129.579                                                          00000270   0
F  ALPHA                                                                         00000280   0
M  IP                                                                            00000290   0
B    130.000    157.000                                                          00000300   0
M  IPH                                                                           00000310   0
B    130.000    157.000                                                          00000320   0
M  IP                                                                            00000330   0
E    157.000    203.000                                                          00000340   0
M  IPH                                                                           00000350   0
B    157.000    203.000                                                          00000360   0
M  IP                                                                            00000370   0
E    203.000    255.000                                                          00000380   0
M  IPH                                                                           00000390   0
B    203.000    255.000                                                          00000400   0
M  IP                                                                            00000410   0
B    255.000    287.000                                                          00000420   0
M  IPH                                                                           00000430   0
E    255.000    287.000                                                          00000440   0
M  IP                                                                            00000450   0
E    287.000    335.000                                                          00000460   0
M  IPH                                                                           00000470   0
E    287.000    335.000                                                          00000480   0
M  IP                                                                            00000490   0
B    335.000    408.000                                                          00000500   0
M  IPH                                                                           00000510   0
E    335.000    408.000                                                          00000520   0
M  IP                                                                            00000530   0
E    408.000    530.000                                                          00000540   0
M  IPH                                                                           00000550   0
B    408.000    530.000                                                          00000560   0
M  IP                                                                            00000570   0
E    530.000    767.000                                                          00000580   0
M  IPH                                                                           00000590   0
E    530.000    767.000                                                          00000600   0
F  PROTON                                                                        00000610   0
M  IA2                                                                           00000620   0
E    4.05        6.000                                                           00000630   0
M  IA3                                                                           00000640   0
B    6.340      10.260                                                           00000650   0
B    10.260     16.420                                                           00000660   0
B    16.420     27.560                                                           00000670   0
M  IB2                                                                           00000680   0
B    17.880     26.70                                                            00000690   0
M  MEAN                                                                         X00000700
                                           IA3    IB3                            00000710   0
E    27.740     42.100                                                           00000720   0
B    42.100     54.400                                                           00000730   0
M  IB3                                                                           00000740   0
```

Table 13. FLUXPLOT Card Input
(2 of 2)

```
      56.800    65.400                                          00000750          0
M IPY                                                           00000760          0
E     76.620    86.020                                          00000770          0
M IPH                                                           00000780          0
E    132.0     155.0                                            00000790          0
E    155.0     175.0                                            00000800          0
E    175.0     203.0                                            00000810          0
E    203.0     220.0                                            00000820          0
E    220.0     242.000                                          00000830          0
E    242.000   270.0                                            00000840          0
E    270.0     303.000                                          00000850          0
E    303.000   346.0                                            00000860          0
E    346.000   407.0                                            00000870          0
```

ISEE-3 999 DAY 0 HR 0 MIN 0 SEC SUMMARY BEGINNING AT 78/11/24 0: 0: 0

DATA TYPE	UNCHECKED COUNTS	UNCHECKED ACCUM TIME	TREND CHECKED COUNTS	TREND CHECKED ACCUM TIME	RATE	NUMBER OF EVENTS	LIVE-TIME
5-FET I AST. HIGH GAIN	54369	6.1533E 05	52492	5.9290E 05	8.8535E-02	44298	5.0035E 05
7-FET I DEEP, HIGH GAIN	35935	4.6154E 05	35876	4.6088E 05	7.7845E-02	30720	3.9463E 05
9-FET I AST, LOW GAIN	17592	6.1898E 05	9052	5.9514E 05	1.5210E-02	9259	6.0678E 05
10-FET I PEN. HIGH GAIN	383725	6.1504E 05	365630	5.9270E 05	6.2357E-01	190413	3.0516E 05
11-FET I PEN. LOW GAIN	65536	6.1878E 05	62907	5.9498E 05	1.0573E-01	56671	5.5491E 05

BIN DEFINITION	DATA TYPE	EVENT COUNT	NORMALIZED COUNTS	LIVE-TIME	FLUX	ERROR
4.39- [illegible] MEV HE4	5	26	2.0663E 01	500345.	3.9386E-05	7.7241E-06
6.39- 10.15 MEV HE4	5	20	1.7057E 01	500345.	9.0383E-06	2.0204E-06
10.16- 16.38 MEV HE4	5	25	1.9639E 01	500345.	6.3136E-06	1.2627E-06
16.38- 27.33 MEV HE4	5	57	4.6104E 01	500345.	8.4111E-06	1.1141E-06
20.24- 26.79 MEV HE4	7	101	8.5936E 01	394630.	3.3241E-05	3.3076E-06
19.28- 26.36 MEV HE4	7	98	8.4153E 01	394630.	3.0128E-05	3.0434E-06
19.28- 26.36 MEV HE4	9	3	1.7830E 00	608746.	4.1381E-07	2.3891E-07
26.25- 42.29 MEV HE4	5	42	3.8879E 01	500345.	8.5505E-06	9.1824E-07
26.25- 42.29 MEV HE4	7	84	5.2828E 01	394630.	1.0263E-05	1.1198E-06
42.25- 56.53 MEV HE4	5	27	2.8693E 01	500345.	4.0275E-06	7.7510E-07
42.29- 56.53 MEV HE4	7	65	5.2190E 01	394630.	9.2883E-06	1.1182E-06
26.19- 42.67 MEV HE4	7	83	5.2220E 01	394630.	9.8164E-06	1.0775E-06
26.19- 42.67 MEV HE4	9	160	1.0208E 02	608746.	1.2440E-05	9.8347E-07
42.67- 56.81 MEV HE4	7	68	5.1336E 01	394630.	9.2041E-06	1.1162E-06
42.67- 56.81 MEV HE4	9	155	1.1913E 02	608746.	1.2846E-05	1.1121E-06
56.81- 69.52 MEV HE4	7	51	4.8657E 01	394630.	9.7012E-06	1.3584E-06
56.81- 69.52 MEV HE4	9	55	9.0959E 01	608746.	1.1757E-05	1.2062E-06
ALL-PENETRATING ALPHA MODES HAVE THEIR GEOMETRY FACTORS CORRECTED FOR NUCLEAR INTERACTIONS : /1.12						
80.52-101.24 MEV ALPHA	11	106	1.4070E 02	554912.	1.2241E-05	1.1890E-06
96.42-112.12 MEV ALPHA	10	66	8.6276E 01	305163.	1.6616E-05	2.2346E-06
112.12-129.58 MEV ALPHA	10	85	1.1282E 02	305163.	2.1173E-05	2.2566E-06
124.18-156.95 MEV ALPHA	11	599	7.9751E 02	554912.	2.1658E-05	8.9309E-07
129.58-156.56 MEV ALPHA	10	266	1.7653E 02	305163.	2.1440E-05	1.3146E-06
156.95-200.60 MEV ALPHA	11	808	5.3620E 02	554912.	2.2138E-05	7.7883E-07
156.56-202.13 MEV ALPHA	10	445	2.9532E 02	305163.	2.1236E-05	1.0067E-06
200.60-251.08 MEV ALPHA	11	617	6.0953E 02	554912.	2.1724E-05	7.1738E-07
202.13-254.08 MEV ALPHA	10	520	3.4509E 02	305163.	2.1767E-05	9.5456E-07
251.08-286.04 MEV ALPHA	11	611	4.0547E 02	554912.	2.0659E-05	8.4550E-07
254.08-284.15 MEV ALPHA	10	328	2.1768E 02	305163.	2.3720E-05	1.3097E-06
286.04-334.08 MEV ALPHA	11	914	6.0654E 02	554912.	2.2754E-05	7.5265E-07
284.15-334.06 MEV ALPHA	10	481	3.1921E 02	305163.	2.0959E-05	9.5563E-07
334.08-405.44 MEV ALPHA	11	1240	8.2286E 02	554912.	2.0780E-05	5.9011E-07
334.06-407.27 MEV ALPHA	10	674	4.4728E 02	305163.	2.0022E-05	7.7122E-07
405.44-519.56 MEV ALPHA	11	1696	1.1255E 03	554912.	1.7773E-05	4.3155E-07
407.27-527.22 MEV ALPHA	10	1041	6.9081E 02	305163.	1.8872E-05	5.8491E-07
519.56-777.09 MEV ALPHA	11	2582	1.7134E 03	554912.	1.4194E-05	2.7934E-07
527.22-76[illegible] MEV ALPHA	10	1808	1.1998E 03	305163.	1.6300E-05	3.8567E-07
4.43- [illegible] MEV PROTON	5	480	5.3196E 02	500345.	6.2[illegible]E-04	3.0792E-05

Table 14. FLUXPLOT Output (1 of 2)

Table 14. FLUXPLOT Output (2 of 2)

6.39- 10.81	MEV	PROTON	5	130	1.0128E 02	500345.	4.5778E-05	5.0150E-06
10.81- 16.77	MEV	PROTON	5	72	5.6096E 01	500345.	1.6618E-05	2.2177E-06
16.77- 28.06	MEV	PROTON	5	109	8.1893E 01	500345.	1.4497E-05	1.4284E-06
20.24- 24.80	MEV	PROTON	7	145	1.0114E 02	394630.	5.9764E-05	3.3022E-06
29.37- 42.27	MEV	PROTON	5	150	1.7565E 02	500345.	2.1019E-05	1.7158E-06
29.37- 42.27	MEV	PROTON	7	210	1.7261E 02	394630.	2.6047E-05	1.7974E-06
42.27- 54.72	MEV	PROTON	5	59	6.1734E 01	500345.	9.9146E-06	1.2908E-06
42.27- 54.72	MEV	PROTON	7	200	1.6177E 02	394630.	3.0904E-05	2.1852E-06
56.54- 70.07	MEV	PROTON	7	193	1.5771E 02	394630.	5.6613E-05	2.6210E-06
76.62- 84.63	MEV	PROTON	10	105	1.2444E 02	305163.	5.0914E-05	4.5687E-06
126.63-154.32	MEV	PROTON	10	1425	8.4436E 02	305163.	9.9936E-05	2.6474E-06
154.32-174.24	MEV	PROTON	10	1036	6.1387E 02	305163.	1.0099E-04	3.1377E-06
174.24-202.00	MEV	PROTON	10	1546	9.1606E 02	305163.	1.0812E-04	2.7497E-06
202.00-215.76	MEV	PROTON	10	1102	6.5297E 02	305163.	1.2048E-04	3.6294E-06
215.76-241.23	MEV	PROTON	10	1351	8.0064E 02	305163.	1.2312E-04	3.3373E-06
241.23-265.29	MEV	PROTON	10	1547	9.1665E 02	305163.	1.0702E-04	2.7208E-06
265.29-302.26	MEV	PROTON	10	1947	1.1537E 03	305163.	1.1466E-04	2.5989E-06
302.26-345.24	MEV	PROTON	10	2655	1.5732E 03	305163.	1.1594E-04	2.3278E-06
345.24-406.33	MEV	PROTON	10	4054	2.4021E 03	305163.	1.2586E-04	2.0239E-06

Table 15 FLUXPLOT Program Time Input for ISEE-3

```
//  EXEC  FLUXPLOT,REG=800K
//*45678901234567890123456789012345678901234567890123456789012345678901234567890123456789
//FLUXPLOT.CARDS DD *,DCB=BLKSIZE=800
S ISEE-3                  999:00:00:00       0 096  TTF  FFT  TFT  I
SI        78/11/24 00:00:00 79/02/03 00:00:00
SE        78/11/29 00:00:00 78/12/08 00:00:00
SE        78/12/11 00:00:00 79/01/17 00:00:00
SE        79/01/21 00:00:00 79/01/27 00:00:00
SE        79/01/30 00:00:00 79/01/31 00:00:00
```

7 18 days of data

```
//  EXEC  FLUXPLOT,REG=800K
//*45678901234567890123456789012345678901234567890123456789012345678901234567890123456789
//FLUXPLOT.CARDS DD *,DCB=BLKSIZE=800
S ISEE-3                  999:00:00:00       0 096  TTF  FFT  TFT  I
SI        79/10/01 00:00:00 79/12/15 00:00:00
SE        79/11/14 00:00:00 79/11/18 00:00:00
```

```
//  EXEC  FLUXPLOT,REG=800K
//*45678901234567890123456789012345678901234567890123456789012345678901234567890123456789
//FLUXPLOT.CARDS DD *,DCB=BLKSIZE=800
S ISEE-3                  999:00:00:00       0 096  TTF  FFT  TFT  I
SI        80/12/01 00:00:00 81/02/01 00:00:00
```

```
//  EXEC  FLUXPLOT,REG=800K
//*45678901234567890123456789012345678901234567890123456789012345678901234567890123456789
//FLUXPLOT.CARDS DD *,DCB=BLKSIZE=800
S ISEE-3                  999:00:00:00       0 096  TTF  FFT  TFT  I
SI        82/04/01 00:00:00 82/06/01 00:00:00
```

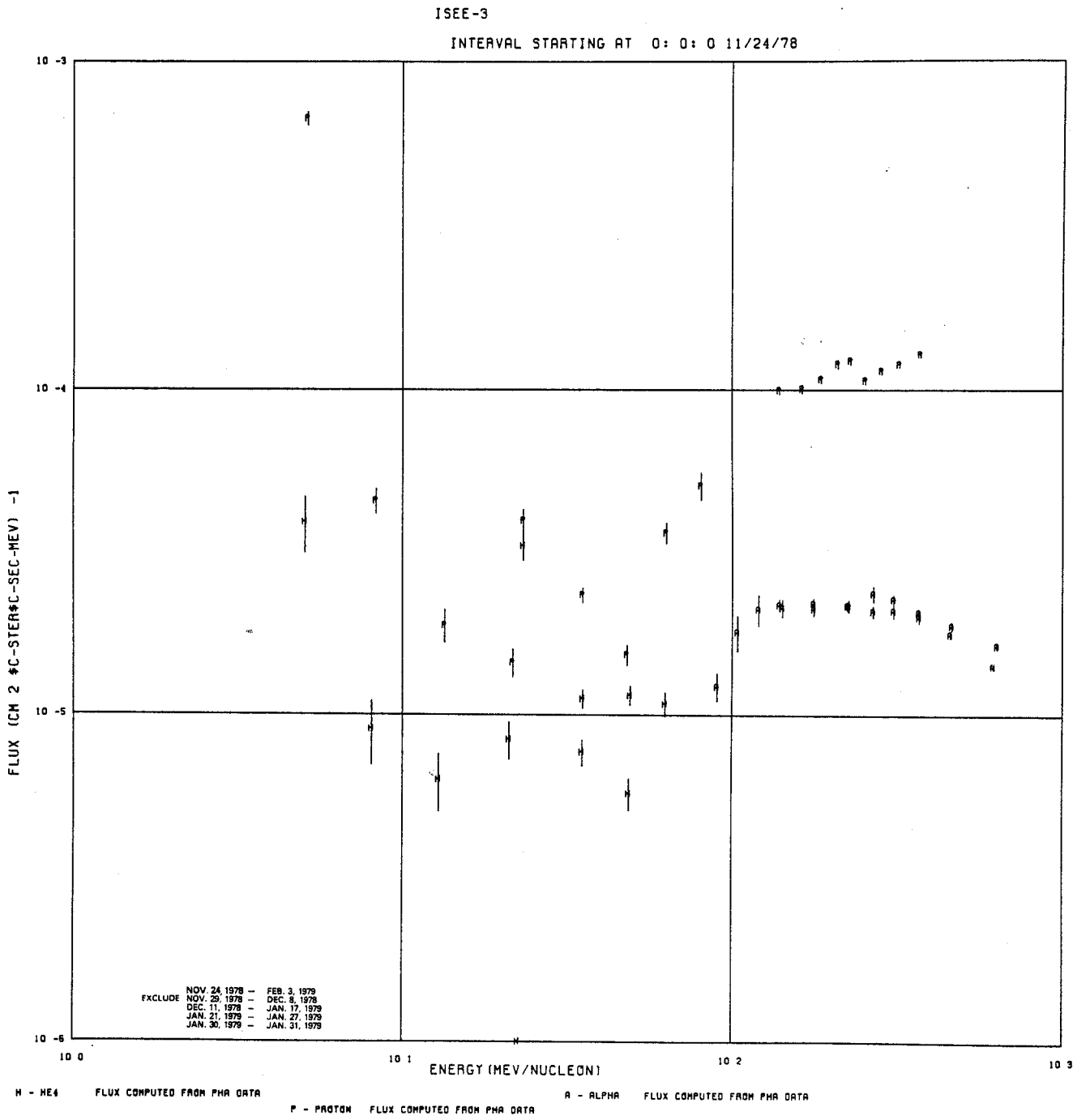

Figure 5. ISEE-3 Fluxes for the Period November 24, 1978 to February 3, 1979

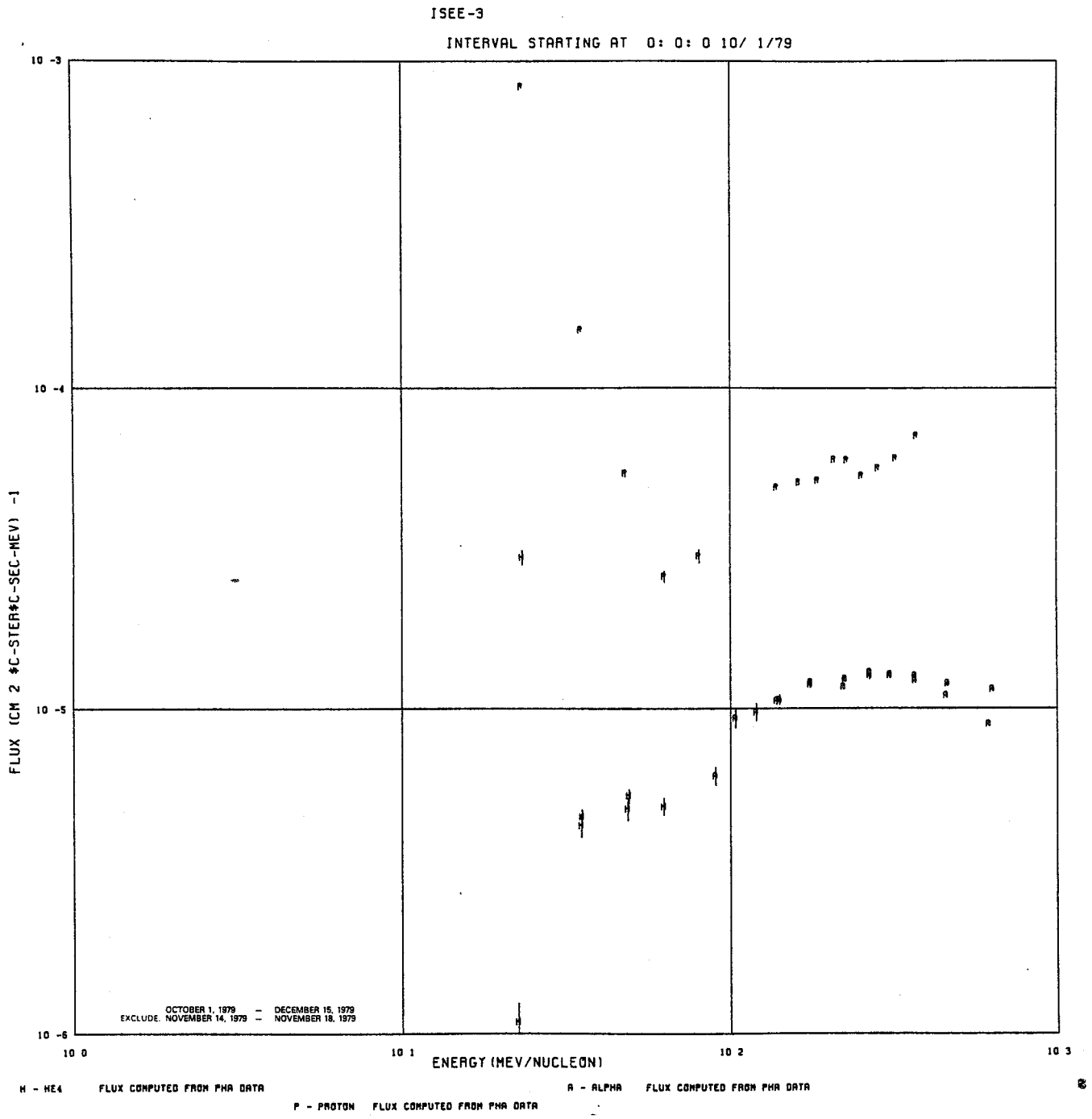

Figure 6. ISEE-3 Fluxes for the Period October 1 December 15, 1979

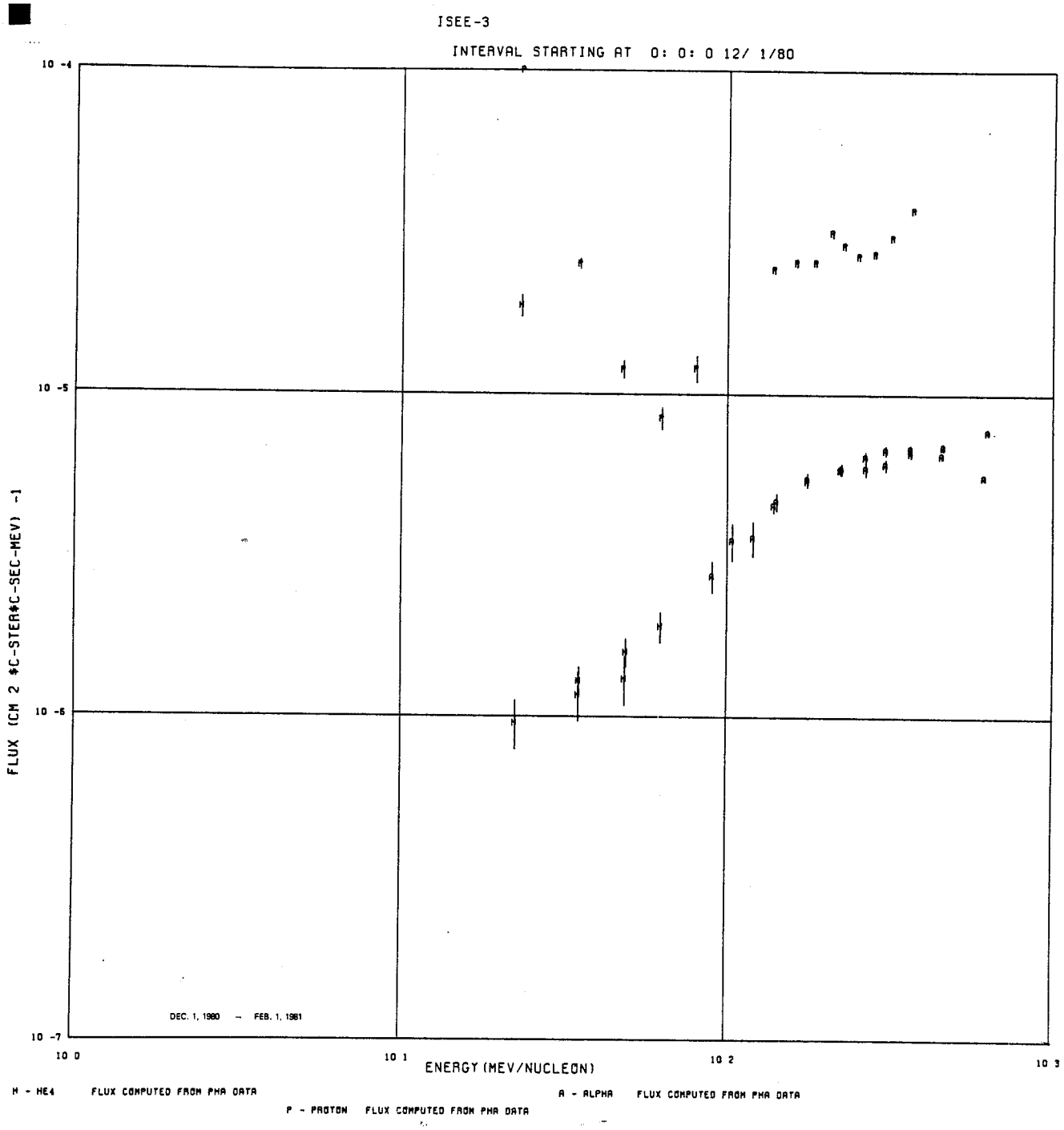

Figure 7. ISEE-3 Fluxes for the Period December 1, 1980 to February 1, 1981

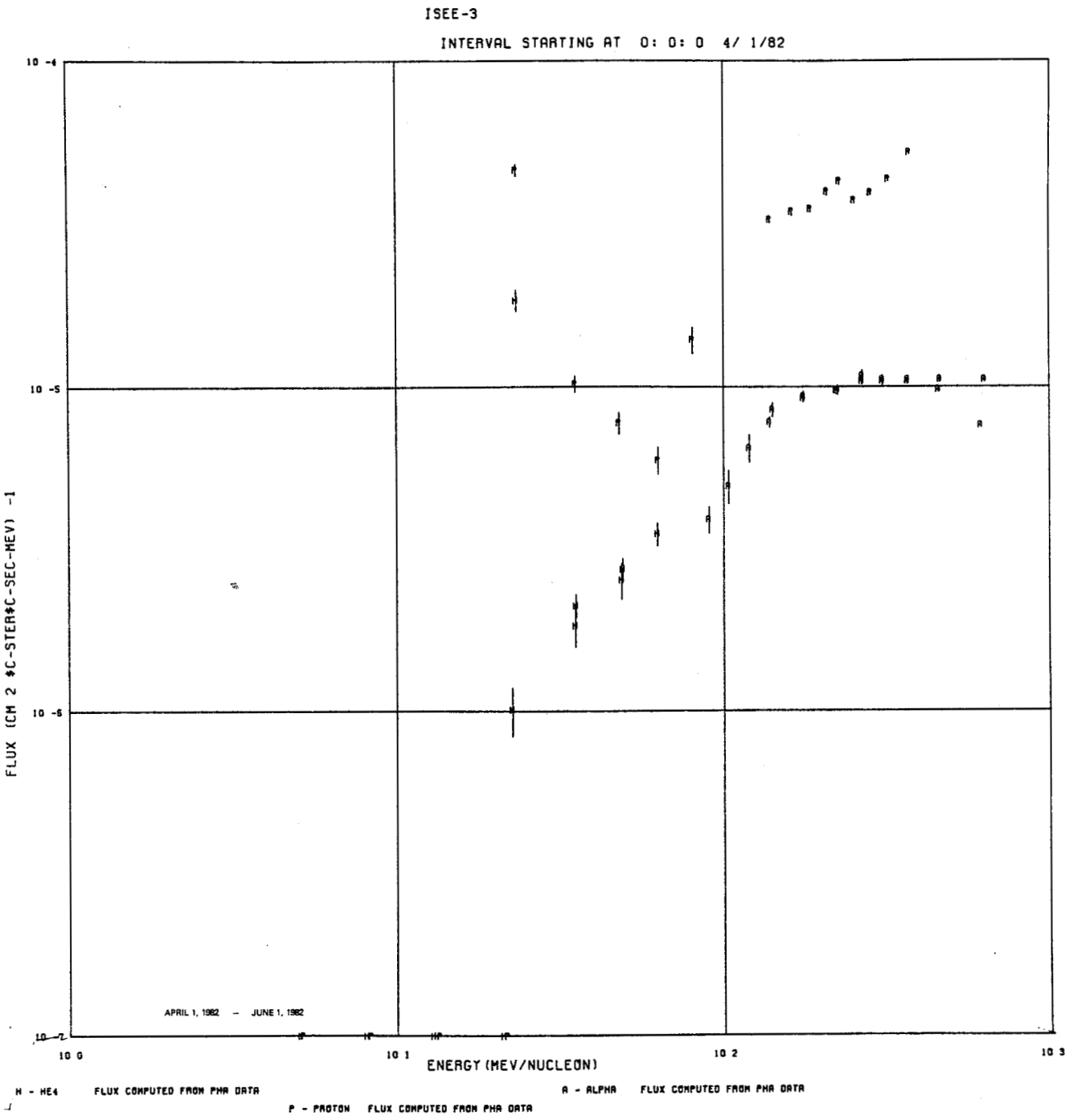

Figure 8. ISEE-3 Fluxes for the Period April 1, 1982 to June 1, 1982

4.3 ISEE-3 HET RESPONSE MODE INFORMATION SUMMARY (PROTONS, HE4(ALPHA))

This section summarizes existing ISEE-3 response modes for proton and alpha particles along with their associated event types and energy ranges. Dead layer ranges are enumerated as are the overlapping energy regions among the various two- and three- dimensional modes.

4.3.1 ALPHA

	Description				Mode	Energy Range		Event Type
HET-1	3-PARAM	LOW	GAIN	B-PEN	IP	101.236	2400.201	11
HET-1	3-PARAM	LOW	GAIN	B-PEN	IPB	80.524	101.236	11
HET-1	3-PARAM	HIGH	GAIN	B-PEN	IPH	129.579	2400.201	10
HET-1	3-PARAM	HIGH	GAIN	B-PEN	IPY	96.425	129.579	10

HET-2 No calibrated responses exist for penetrating modes

4.3.2 HE4

HET-1	2-PARAM	HIGH	GAIN	A-STOP	IA2	4.350	6.598	5
HET-1	3-PARAM	HIGH	GAIN	A-STOP	IA3	6.390	58.558	5
HET-1	2-PARAM	HIGH	GAIN	B-STOP	IB2	20.238	29.508	7
HET-1	3-PARAM	HIGH	GAIN	B-STOP	IB3	29.122	70.944	7
HET-2	3-PARAM	HIGH	GAIN	A-STOP	IIA3	6.438	58.780	12
HET-2	2-PARAM	HIGH	GAIN	A-STOP	IIA2	4.362	6.649	12
HET-2	2-PARAM	HIGH	GAIN	B-STOP	IIB2	19.293	29.063	14

HET-2	3-PARAM	HIGH GAIN	B-STOP		IIB3	28.708	70.908	
HET-2	2-PARAM	LOW GAIN	B-STOP	Z > 1	IIL2	18.260	26.976	16
HET-2	3-PARAM	LOW GAIN	B-STOP	Z > 1	IIL3	28.773	70.957	16
HET-1	2-PARAM	LOW GAIN	B-STOP	Z > 1	IL2	18.328	27.039	9
HET-1	3-PARAM	LOW GAIN	B-STOP	Z > 1	IL3	29.186	70.979	9

4.3.3 PROTON

HET-1	2-PARAM	HIGH GAIN	A-STOP	IA2	4.432	6.627	5
HET-1	3-PARAM	HIGH GAIN	A-STOP	IA3	6.386	58.356	5
HET-1	2-PARAM	HIGH GAIN	B-STOP	IB2	20.360	29.402	7
HET-1	3-PARAM	HIGH GAIN	B-STOP	IB3	29.052	70.675	7
HET-2	2-PARAM	HIGH GAIN	A-STOP	IIA2	4.447	6.652	12
HET-2	3-PARAM	HIGH GAIN	A-STOP	IIA3	6.469	58.577	12
HET-2	2-PARAM	HIGH GAIN	B-STOP	IIB2	19.443	28.967	14
HET-2	3-PARAM	HIGH GAIN	B-STOP	IIB3	28.641	70.651	14
HET-1	3-PARAM	HIGH GAIN	B-PEN	IPH	121.563	2400.200	10
HET-1	3-PARAM	HIGH GAIN	B-PEN	IPY	76.617	86.023	10

4.3.4 OVERLAPPING MODES BY ENERGY REGION

PROTON

4.45 - 6.63 Mev	IA2,IIA2
6.47 - 58.36 Mev	IA3,IIA3
20.36- 28.97 Mev	IA3,IIA3,IE2,IIE2
29.05- 58.36 Mev	IA3,IIA3,IE3,IIE3
29.05- 70.65 Mev	IE3,IIB3

ALPHA and HE4

4.36 - 6.60 Mev	IA2,IIA2
6.44 - 58.56 Mev	IA3,IIA3
20.24- 26.98 Mev	IA3,IIA3,IE2,IIE2,IL2,IIL2
29.19- 58.56 Mev	IA3,IIA3,IE3,IIE3,IL3,IIL3
29.19- 58.56 Mev	IE3,IIE3,IL3,IIL3
96.42-101.24 Mev	IEB,IEY
129.58-2400.20 Mev	IP,IPH

4.3.5 DEAD LAYER RANGES

These ranges are multi-valued regions and should not be split into parts when doing bin requests for FLUXPLOT.

Mode	Particle	Dead-Layer-Energies	
IA3	PROTON	21-27	
		30-38	
		44-59	
IA3	He4	21-26	
		30-36	
		46-55	
IL3	He4	34-39	B-Stopping
		48-54	
		60-70	
IB3	PROTON	33-38	
		48-54	
		60-70	
IE3	He4	34-38	
		48-53	
		60-70	

Mode	Particle	Dead-Layer-Energies	
IIA3	PROTON	21-26	
		30-38	
		44-59	
IIA3	He4	21-26	
		30-38	
		46-59	
IIL3	He4	34-38	B-Stopping
		48-53	
		60-70	
IIB3	PROTON	33-38	
		48-53	
		59-70	
IIB3	He4	34-38	
		48-53	
		60-70	

4.4 ISEE-3 HET RESPONSE MODE INFORMATION SUMMARY (CONTINUED)

Stopping modes for elements with atomic number greater than 2 are listed in this section. Responses for HE3, Deuteron, and Electron particle types are also included here.

4.4.1 AL27

Description						Mode	Energy Range		Event Type
HET-1	2-PARAM	LOW	GAIN	A-STOP	Z > 2	IA2	11.025	17.897	6
HET-1	3-PARAM	LOW	GAIN	A-STOP	Z > 2	IA3	16.849	165.891	6
HET-1	3-PARAM	LOW	GAIN	B-STOP	Z > 1	IB3	81.027	202.617	9
HET-2	3-PARAM	LOW	GAIN	A-STOP	Z > 2	IIA3	16.948	166.545	13
HET-2	2-PARAM	LOW	GAIN	A-STOP	Z > 2	IIA2	11.070	17.967	13
HET-2	3-PARAM	LOW	GAIN	B-STOP	Z > 1	IIB3	79.856	202.640	16

4.4.2 AR36

HET-1	2-PARAM	LOW	GAIN	A-STOP	Z > 2	IA2	13.106	21.539	6
HET-1	3-PARAM	LOW	GAIN	A-STOP	Z > 2	IA3	20.233	204.982	6
HET-1	3-PARAM	LOW	GAIN	B-STOP	Z > 1	IB3	99.285	251.295	9
HET-2	3-PARAM	LOW	GAIN	A-STOP	Z > 2	IIA3	20.355	205.802	13
HET-2	2-PARAM	LOW	GAIN	A-STOP	Z > 2	IIA2	13.161	21.668	13
HET-2	3-PARAM	LOW	GAIN	B-STOP	Z > 1	IIB3	97.837	251.084	16

4.4.3 BE9

HET-1	2-PARAM	LOW	GAIN	A-STOP	Z > 2	IA2	5.914	9.157	6
HET-1	3-PARAM	LOW	GAIN	A-STOP	Z > 2	IA3	8.763	80.939	6
HET-1	3-PARAM	LOW	GAIN	B-STOP	Z > 1	IB3	40.179	98.196	9
HET-2	2-PARAM	LOW	GAIN	A-STOP	Z > 2	IIA2	5.936	9.265	13
HET-2	3-PARAM	LOW	GAIN	A-STOP	Z > 2	IIA3	8.811	81.248	13
HET-2	3-PARAM	LOW	GAIN	B-STOP	Z > 1	IIB3	39.608	98.184	16

4.4.4 B11

HET-1	2-PARAM	LOW	GAIN	A-STOP	Z > 2	IA2	6.723	10.530	6
HET-1	3-PARAM	LOW	GAIN	A-STOP	Z > 2	IA3	9.999	92.972	6
HET-1	3-PARAM	LOW	GAIN	B-STOP	Z > 1	IB3	46.069	112.913	9
HET-2	3-PARAM	LOW	GAIN	A-STOP	Z > 2	IIA3	10.054	93.329	13
HET-2	2-PARAM	LOW	GAIN	A-STOP	Z > 2	IIA2	6.748	10.559	13
HET-2	3-PARAM	LOW	GAIN	B-STOP	Z > 1	IIB3	45.413	112.834	16

4.4.5 CA40

HET-1	2-PARAM	LOW	GAIN	A-STOP	Z > 2	IA2	13.765	22.707	6
HET-1	3-PARAM	LOW	GAIN	A-STOP	Z > 2	IA3	21.322	218.097	6
HET-1	2-PARAM	LOW	GAIN	B-STOP	Z > 1	IB2	65.391	97.701	9
HET-1	3-PARAM	LOW	GAIN	B-STOP	Z > 1	IB3	105.335	267.637	9
HET-2	2-PARAM	LOW	GAIN	A-STOP	Z > 2	IIA2	13.824	22.844	13
HET-2	3-PARAM	LOW	GAIN	A-STOP	Z > 2	IIA3	21.451	218.973	13
HET-2	2-PARAM	LOW	GAIN	B-STOP	Z > 1	IIB2	65.148	97.430	16
HET-2	3-PARAM	LOW	GAIN	B-STOP	Z > 1	IIB3	103.794	267.453	16

4.4.6 CR52

HET-1	2-PARAM	LOW	GAIN	A-STOP	Z > 2	IA2	13.901	23.361	6
HET-1	3-PARAM	LOW	GAIN	A-STOP	Z > 2	IA3	21.893	231.470	6
HET-1	3-PARAM	LOW	GAIN	B-STOP	Z > 1	IB3	111.241	284.532	9
HET-2	2-PARAM	LOW	GAIN	A-STOP	Z > 2	IIA2	13.963	23.506	13
HET-2	3-PARAM	LOW	GAIN	A-STOP	Z > 2	IIA3	22.030	232.406	13
HET-2	3-PARAM	LOW	GAIN	B-STOP	Z > 1	IIB3	109.600	284.412	16

4.4.7 C12

HET-1	2-PARAM	LOW	GAIN	A-STOP	Z > 2	IA2	7.822	12.330	6
HET-1	3-PARAM	LOW	GAIN	A-STOP	Z > 2	IA3	11.647	108.826	6
HET-1	2-PARAM	LOW	GAIN	B-STOP	Z > 1	IB2	33.793	49.940	9
HET-1	3-PARAM	LOW	GAIN	B-STOP	Z > 1	IB3	53.795	132.296	9
HET-2	2-PARAM	LOW	GAIN	A-STOP	Z > 2	IIA2	7.851	12.390	13
HET-2	3-PARAM	LOW	GAIN	A-STOP	Z > 2	IIA3	11.712	109.246	13
HET-2	2-PARAM	LOW	GAIN	B-STOP	Z > 1	IIB2	33.671	49.806	16
HET-2	3-PARAM	LOW	GAIN	B-STOP	Z > 1	IIB3	53.028	132.222	16

4.4.8 DEUTRON

HET-1	2-PARAM	HIGH	GAIN	A-STOP		IA2	2.926	4.461	5
HET-1	3-PARAM	HIGH	GAIN	A-STOP		IA3	4.259	39.591	5
HET-1	2-PARAM	HIGH	GAIN	B-STOP		IB2	13.731	19.940	7
HET-1	3-PARAM	HIGH	GAIN	B-STOP		IB3	19.694	47.926	7
HET-2	2-PARAM	HIGH	GAIN	A-STOP		IIA2	2.936	4.433	12
HET-2	3-PARAM	HIGH	GAIN	A-STOP		IIA3	4.305	39.741	12
HET-2	2-PARAM	HIGH	GAIN	B-STOP		IIB2	13.100	19.636	14
HET-2	3-PARAM	HIGH	GAIN	B-STOP		IIB3	19.414	47.895	14

4.4.9 ELEC

HET-1	2-PARAM	HIGH	GAIN	A-STOP		IA2	0.220	2.000	5
HET-2	2-PARAM	HIGH	GAIN	A-STOP		IIA2	0.220	2.000	12

4.4.10 FE56

HET-1	2-PARAM	LOW	GAIN	A-STOP	Z > 2	IA2	14.375	24.286	6
HET-1	3-PARAM	LOW	GAIN	A-STOP	Z > 2	IA3	22.745	243.531	6
HET-1	2-PARAM	LOW	GAIN	B-STOP	Z > 1	IB2	72.017	108.168	9
HET-1	3-PARAM	LOW	GAIN	B-STOP	Z > 1	IB3	116.678	299.633	9
HET-2	2-PARAM	LOW	GAIN	A-STOP	Z > 2	IIA2	14.439	24.437	13
HET-2	3-PARAM	LOW	GAIN	A-STOP	Z > 2	IIA3	22.889	244.522	13
HET-2	2-PARAM	LOW	GAIN	B-STOP	Z > 1	IIB2	71.745	107.859	16
HET-2	3-PARAM	LOW	GAIN	B-STOP	Z > 1	IIB3	114.951	299.538	16

4.4.11 F19

HET-1	2-PARAM	LOW	GAIN	A-STOP	Z > 2	IA2	9.252	14.790	6
HET-1	3-PARAM	LOW	GAIN	A-STOP	Z > 2	IA3	13.934	133.000	6
HET-1	3-PARAM	LOW	GAIN	B-STOP	Z > 1	IB3	65.430	162.037	9
HET-2	3-PARAM	LOW	GAIN	A-STOP	Z > 2	IIA3	14.014	133.517	13
HET-2	2-PARAM	LOW	GAIN	A-STOP	Z > 2	IIA2	9.288	14.874	13
HET-2	3-PARAM	LOW	GAIN	B-STOP	Z > 1	IIB3	64.492	161.946	16

4.4.12 HE3

HET-1	2-PARAM	HIGH	GAIN	A-STOP		IA2	5.127	7.862	5

HET-1	3-PARAM	HIGH GAIN	A-STOP		IA3	7.471	68.648	5
HET-1	2-PARAM	HIGH GAIN	B-STOP		IB2	23.728	34.580	7
HET-1	3-PARAM	HIGH GAIN	B-STOP		IB3	34.123	83.217	7
HET-2	2-PARAM	HIGH GAIN	A-STOP		IIA2	5.145	7.882	12
HET-2	3-PARAM	HIGH GAIN	A-STOP		IIA3	7.523	68.909	12
HET-2	2-PARAM	HIGH GAIN	B-STOP		IIB2	22.623	34.056	14
HET-2	3-PARAM	HIGH GAIN	B-STOP		IIB3	33.639	83.172	14
HET-2	3-PARAM	LOW GAIN	B-STOP	Z > 1	IIL3	33.727	83.208	16

4.4.13 LI6

HET-1	2-PARAM	LOW GAIN	A-STOP	Z > 2	IA2	5.438	8.372	6
HET-1	3-PARAM	LOW GAIN	A-STOP	Z > 2	IA3	8.024	73.567	6
HET-1	3-PARAM	LOW GAIN	B-STOP	Z > 1	IB3	36.567	89.223	9

4.4.14 LI7

HET-2	3-PARAM	LOW GAIN	A-STOP	Z > 2	IIA3	7.375	67.711	13
HET-2	2-PARAM	LOW GAIN	A-STOP	Z > 2	IIA2	4.975	7.793	13
HET-2	3-PARAM	LOW GAIN	B-STOP	Z > 1	IIB3	33.066	81.745	16

4.4.15 MG24

HET-1	2-PARAM	LOW GAIN	A-STOP	Z > 2	IA2	10.902	17.597	6
HET-1	3-PARAM	LOW GAIN	A-STOP	Z > 2	IA3	16.581	161.877	6
HET-1	2-PARAM	LOW GAIN	B-STOP	Z > 1	IB2	49.537	73.526	9
HET-1	3-PARAM	LOW GAIN	B-STOP	Z > 1	IB3	79.163	197.683	9
HET-2	3-PARAM	LOW GAIN	A-STOP	Z > 2	IIA3	16.677	162.513	13
HET-2	2-PARAM	LOW GAIN	A-STOP	Z > 2	IIA2	10.946	17.664	13

HET-2	3-PARAM	LOW	GAIN	B-STOP	Z > 1	IIB3	78.021	197.534	
HET-2	2-PARAM	LOW	GAIN	B-STOP	Z > 1	IIB2	49.356	73.328	16

4.4.16 NA23

HET-1	2-PARAM	LOW	GAIN	A-STOP	Z > 2	IA2	10.247	16.485	6
HET-1	3-PARAM	LOW	GAIN	A-STOP	Z > 2	IA3	15.521	150.059	6
HET-1	3-PARAM	LOW	GAIN	B-STOP	Z > 1	IB3	73.569	183.088	9
HET-2	2-PARAM	LOW	GAIN	A-STOP	Z > 2	IIA2	10.288	16.579	13
HET-2	3-PARAM	LOW	GAIN	A-STOP	Z > 2	IIA3	15.610	150.646	13
HET-2	3-PARAM	LOW	GAIN	B-STOP	Z > 1	IIB3	72.510	182.933	16

4.4.17 NE20

HET-1	2-PARAM	LOW	GAIN	A-STOP	Z > 2	IA2	10.081	16.132	6
HET-1	3-PARAM	LOW	GAIN	A-STOP	Z > 2	IA3	15.196	145.755	6
HET-1	2-PARAM	LOW	GAIN	B-STOP	Z > 1	IB2	44.822	66.406	9
HET-1	3-PARAM	LOW	GAIN	B-STOP	Z > 1	IB3	71.543	177.701	9
HET-2	2-PARAM	LOW	GAIN	A-STOP	Z > 2	IIA2	10.121	16.223	13
HET-2	3-PARAM	LOW	GAIN	A-STOP	Z > 2	IIA3	15.283	146.324	13
HET-2	2-PARAM	LOW	GAIN	B-STOP	Z > 1	IIB2	44.659	66.254	16
HET-2	3-PARAM	LOW	GAIN	B-STOP	Z > 1	IIB3	70.515	177.616	16

4.4.18 NI58

HET-1	2-PARAM	LOW	GAIN	A-STOP	Z > 2	IA2	15.587	25.681	6
HET-1	3-PARAM	LOW	GAIN	A-STOP	Z > 2	IA3	24.801	260.451	
HET-1	3-PARAM	LOW	GAIN	B-STOP	Z > 1	IB3	124.310	320.883	9
HET-2	2-PARAM	LOW	GAIN	A-STOP	Z > 2	IIA2	15.579	25.843	13

HET-2	3-PARAM	LOW	GAIN	A-STOP	Z > 2	IIA3	24.968	261.516	13
HET-2	3-PARAM	LOW	GAIN	B-STOP	Z > 1	IIB3	122.462	320.808	16

4.4.19 N14

HET-1	2-PARAM	LOW	GAIN	A-STOP	Z > 2	IA2	8.468	13.389	6
HET-1	3-PARAM	LOW	GAIN	A-STOP	Z > 2	IA3	12.641	118.807	6
HET-1	2-PARAM	LOW	GAIN	B-STOP	Z > 1	IB2	36.805	54.421	9
HET-1	3-PARAM	LOW	GAIN	B-STOP	Z > 1	IB3	58.625	144.543	9
HET-2	2-PARAM	LOW	GAIN	A-STOP	Z > 2	IIA2	8.500	13.453	13
HET-2	3-PARAM	LOW	GAIN	A-STOP	Z > 2	IIA3	12.712	119.266	13
HET-2	2-PARAM	LOW	GAIN	B-STOP	Z > 1	IIB2	36.672	54.299	16
HET-2	3-PARAM	LOW	GAIN	B-STOP	Z > 1	IIB3	57.787	144.479	16

4.4.20 O16

HET-1	2-PARAM	LOW	GAIN	A-STOP	Z > 2	IA2	9.062	14.376	6
HET-1	3-PARAM	LOW	GAIN	A-STOP	Z > 2	IA3	13.566	128.265	6
HET-1	2-PARAM	LOW	GAIN	B-STOP	Z > 1	IB2	39.639	58.660	9
HET-1	3-PARAM	LOW	GAIN	B-STOP	Z > 1	IB3	63.181	156.158	9
HET-2	2-PARAM	LOW	GAIN	A-STOP	Z > 2	IIA2	9.097	14.445	13
HET-2	3-PARAM	LOW	GAIN	A-STOP	Z > 2	IIA3	13.642	128.762	13
HET-2	2-PARAM	LOW	GAIN	B-STOP	Z > 1	IIB2	39.495	58.497	16
HET-2	3-PARAM	LOW	GAIN	B-STOP	Z > 1	IIB3	62.277	156.103	16

4.4.21 SI28

HET-1	2-PARAM	LOW	GAIN	A-STOP	Z > 2	IA2	11.687	18.993	6
HET-1	3-PARAM	LOW	GAIN	A-STOP	Z > 2	IA3	17.882	177.020	6

HET-1	2-PARAM	LOW	GAIN	B-STOP	Z > 1	IB2	53.899	80.107	9
HET-1	3-PARAM	LOW	GAIN	B-STOP	Z > 1	IB3	86.276	216.415	9
HET-2	2-PARAM	LOW	GAIN	A-STOP	Z > 2	IIA2	11.735	19.127	13
HET-2	3-PARAM	LOW	GAIN	A-STOP	Z > 2	IIA3	17.988	177.720	13
HET-2	2-PARAM	LOW	GAIN	B-STOP	Z > 1	IIB2	53.701	79.880	16
HET-2	3-PARAM	LOW	GAIN	B-STOP	Z > 1	IIB3	85.027	216.291	16

4.4.22 S32

HET-1	2-PARAM	LOW	GAIN	A-STOP	Z > 2	IA2	12.466	20.361	6
HET-1	3-PARAM	LOW	GAIN	A-STOP	Z > 2	IA3	19.139	191.330	6
HET-1	2-PARAM	LOW	GAIN	B-STOP	Z > 1	IB2	57.955	86.292	9
HET-1	3-PARAM	LOW	GAIN	B-STOP	Z > 1	IB3	92.971	234.220	9
HET-2	2-PARAM	LOW	GAIN	A-STOP	Z > 2	IIA2	12.517	20.481	13
HET-2	3-PARAM	LOW	GAIN	A-STOP	Z > 2	IIA3	19.253	192.091	13
HET-2	3-PARAM	LOW	GAIN	B-STOP	Z > 1	IIB3	91.620	234.118	16
HET-2	2-PARAM	LOW	GAIN	B-STOP	Z > 1	IIB2	57.742	86.042	16

4.4.23 TI48

HET-1	2-PARAM	LOW	GAIN	A-STOP	Z > 2	IA2	13.444	22.433	6
HET-1	3-PARAM	LOW	GAIN	A-STOP	Z > 2	IA3	21.039	219.031	6
HET-1	3-PARAM	LOW	GAIN	B-STOP	Z > 1	IB3	105.617	268.890	9
HET-2	2-PARAM	LOW	GAIN	A-STOP	Z > 2	IIA2	13.502	22.570	13
HET-2	3-PARAM	LOW	GAIN	A-STOP	Z > 2	IIA3	21.169	219.912	13
HET-2	3-PARAM	LOW	GAIN	B-STOP	Z > 1	IIB3	104.066	268.747	16

4.4.24 ZN64

HET-1	2-PARAM	LOW	GAIN	A-STOP	Z > 2	IA2	15.443	25.919	6
HET-1	3-PARAM	LOW	GAIN	A-STOP	Z > 2	IA3	24.575	266.545	6
HET-1	3-PARAM	LOW	GAIN	B-STOP	Z > 1	IB3	128.627	328.696	9
HET-2	2-PARAM	LOW	GAIN	A-STOP	Z > 2	IIA2	15.514	26.084	13
HET-2	3-PARAM	LOW	GAIN	A-STOP	Z > 2	IIA3	24.735	267.639	13
HET-2	3-PARAM	LOW	GAIN	B-STOP	Z > 1	IIB3	125.022	328.442	16

APPENDIX A - MATRIX PROGRAM ENDPOINT DETERMINATION

Endpoint determination is described in Section 2.1.1. An example of the technique is illustrated in this appendix. Figure 11 is the plot of the telescope element B1 channel (i.e., pulse height) versus the elements SUM C4C3C2 channel. The actual number of counts for each channel are shown in Figure 12. These counts are summed at each channel to produce Figure 13 , a plot showing a determination of the endpoint channel for elements SUM C4C3C2. The matrix program card input used to generate the endpoint data is shown in Figures 9 and 10.

Matrix data for other endpoints is shown in the following pages.

```
S  ISEE-3                        999 00 00 00                                                00000040    0
SI          78 11 23 00 00 00 79 02 16 00 00 00                                              00000050    0
SE          78 12 10 00 00 00 78 12 16 00 00 00                                              00000060    0
SE          78 12 30 00 00 00 79 01 01 00 00 00                                              00000070    0
SE          79 01 21 00 00 00 79 01 23 00 00 00                                              00000080    0
P  B1   C432          FFTFFFFFFFFFFF                       01  0000 4095                    00000110    0
P  B1   C432          FFTFFFFFFFFFFF                       04  0000 4095                    00000130    0
P  B1   C432          FFTFFFFFFFFFFF                       01  0000 4095                    00000150    0
P  B1   C432          FFTFFFFFFFFFFF                       04  0000 4095                    00000170    0
P  B1   C432          FFTFFFFFFFFFFF                       01  0000 4095                    00000190    0
P  B1   C432          FFTFFFFFFFFFFF                       04  0000 4095                    00000210    0
P  B2   C432          FFTFFFFFFFFFFF                       01  0000 4095                    00000230    0
P  B2   C432          FFTFFFFFFFFFFF                       04  0000 4095                    00000250    0
P  B2   C432          FFTFFFFFFFFFFF                       01  0000 4095                    00000270    0
P  B2   C432          FFTFFFFFFFFFFF                       04  0000 4095                    00000290    0
P  B2   C432          FFTFFFFFFFFFFF                       01  0000 4095                    00000310    0
P  B2   C432          FFTFFFFFFFFFFF                       04  0000 4095                    00000330    0
P  B1   C432          FFFFFFFFF TFFFF                      01  0000 4095                    00000350    0
P  B1   C432          FFFFFFFFF TFFFF                      04  0000 4095                    00000370    0
P  B1   C432          FFFFFFFFF TFFFF                      01  0000 4095                    00000390    0
P  B1   C432          FFFFFFFFF TFFFF                      04  0000 4095                    00000410    0
P  B1   C432          FFFFFFFFF TFFFF                      01  0000 4095                    00000430    0
P  B1   C432          FFFFFFFFF TFFFF                      04  0000 4095                    00000450    0
P  B2   C432          FFFFFFFFF TFFFF                      01  0000 4095                    00000470    0
P  B2   C432          FFFFFFFFF TFFFF                      04  0000 4095                    00000490    0
P  B2   C432          FFFFFFFFF TFFFF                      01  0000 4095                    00000510    0
P  B2   C432          FFFFFFFFF TFFFF                      04  0000 4095                    00000530    0
P  B2   C432          FFFFFFFFF TFFFF                      01  0000 4095                    00000550    0
P  B2   C432          FFFFFFFFF TFFFF                      04  0000 4095                    00000570    0
```

Figure 9.   Endpoint Data Card Input for MATRIX High Gain, B-Stopping

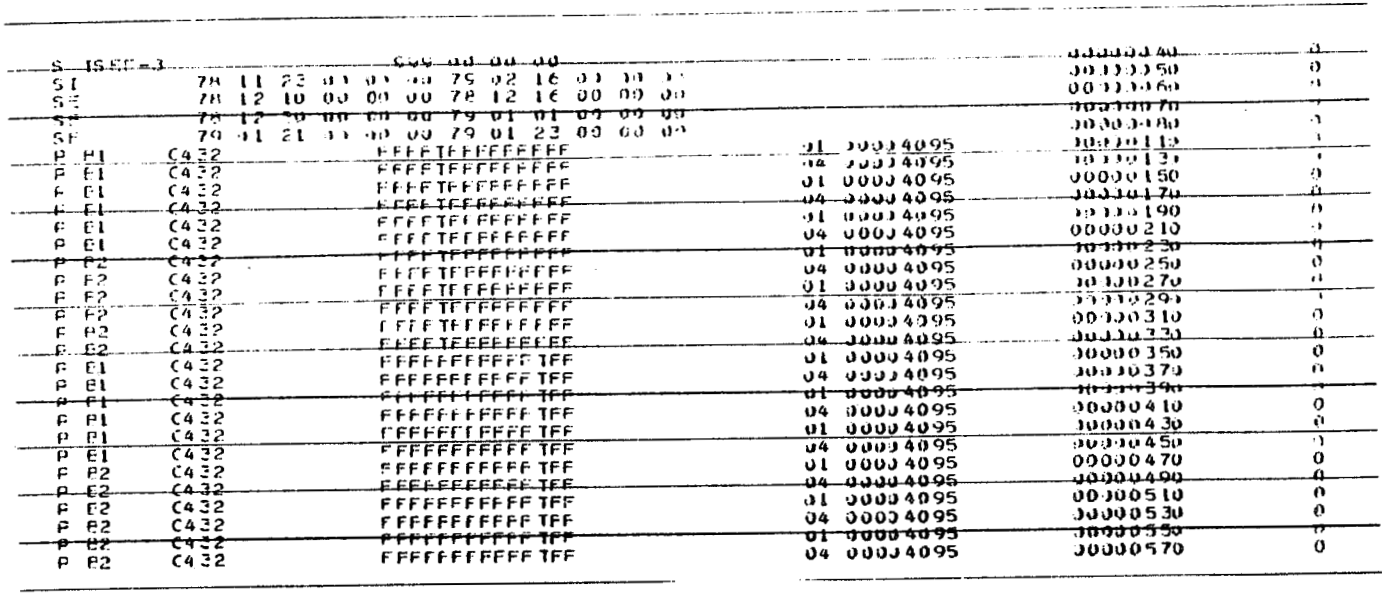

Figure 10. Endpoint Data Card Input for MATRIX Low Gain, B-Stopping

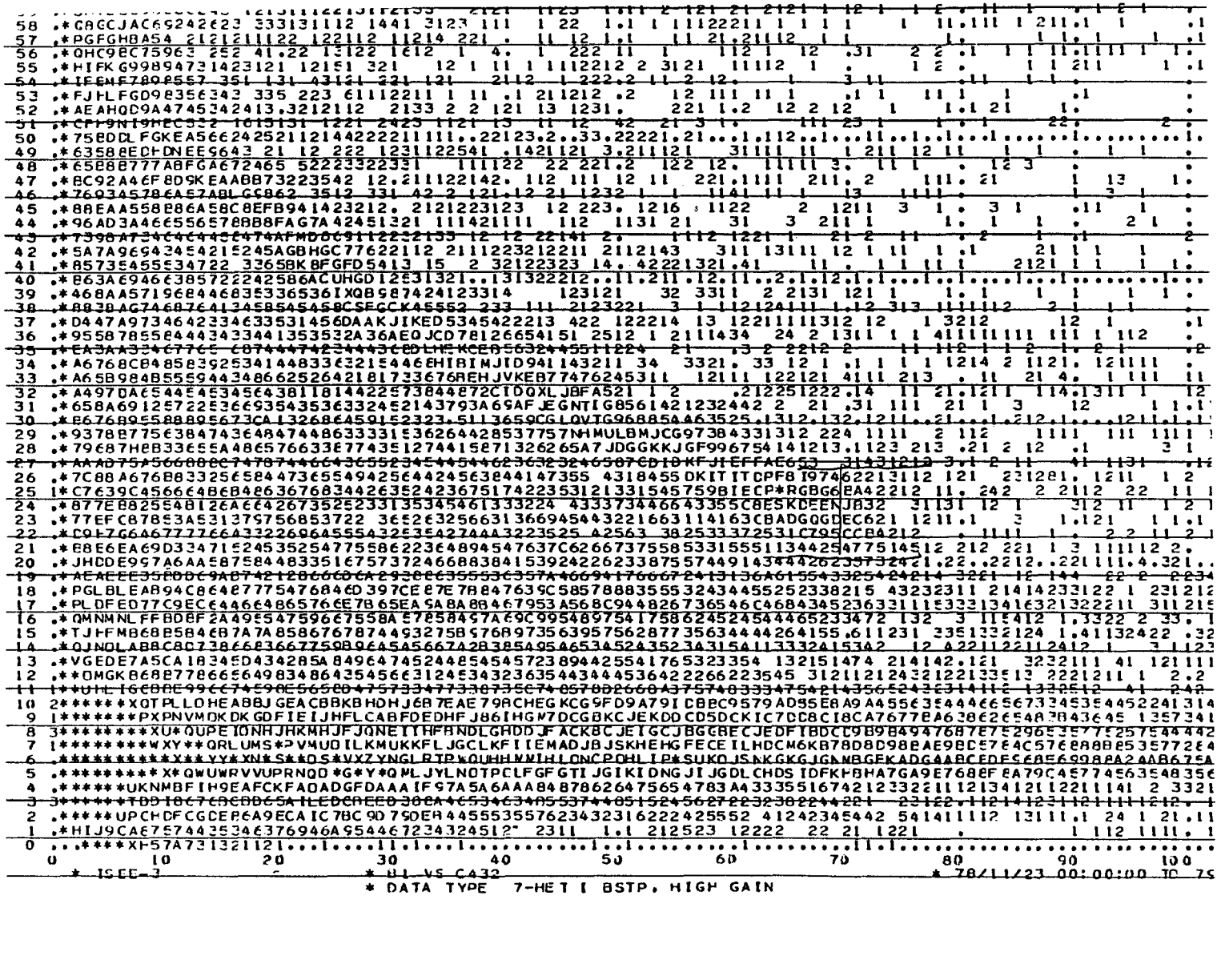

Figure 11. Data Plot for Mode 7-IBSP

ISEE-3

26	8	18	9	7	4	6	2	2	1	3	1	1	2
25	27	16	11	16	6	11	10	4	2	2	1	2	-
24	20	13	14	14	23	19	11	3	2	-	-	3	1
23	13	16	26	16	13	14	12	6	2	1	-	1	2
22	1	12	7	9	5	12	12	11	4	2	1	2	-
21	3	4	4	2	5	4	7	7	5	1	4	5	1
20	4	4	2	6	2	3	3	7	3	2	4	2	1
	65	66	67	68	69	70	71	72	73	74	75	76	77

IBSP 7, B1 vs C432
78/11/23 79/02/16

Figure 12. Data from Mass Line End

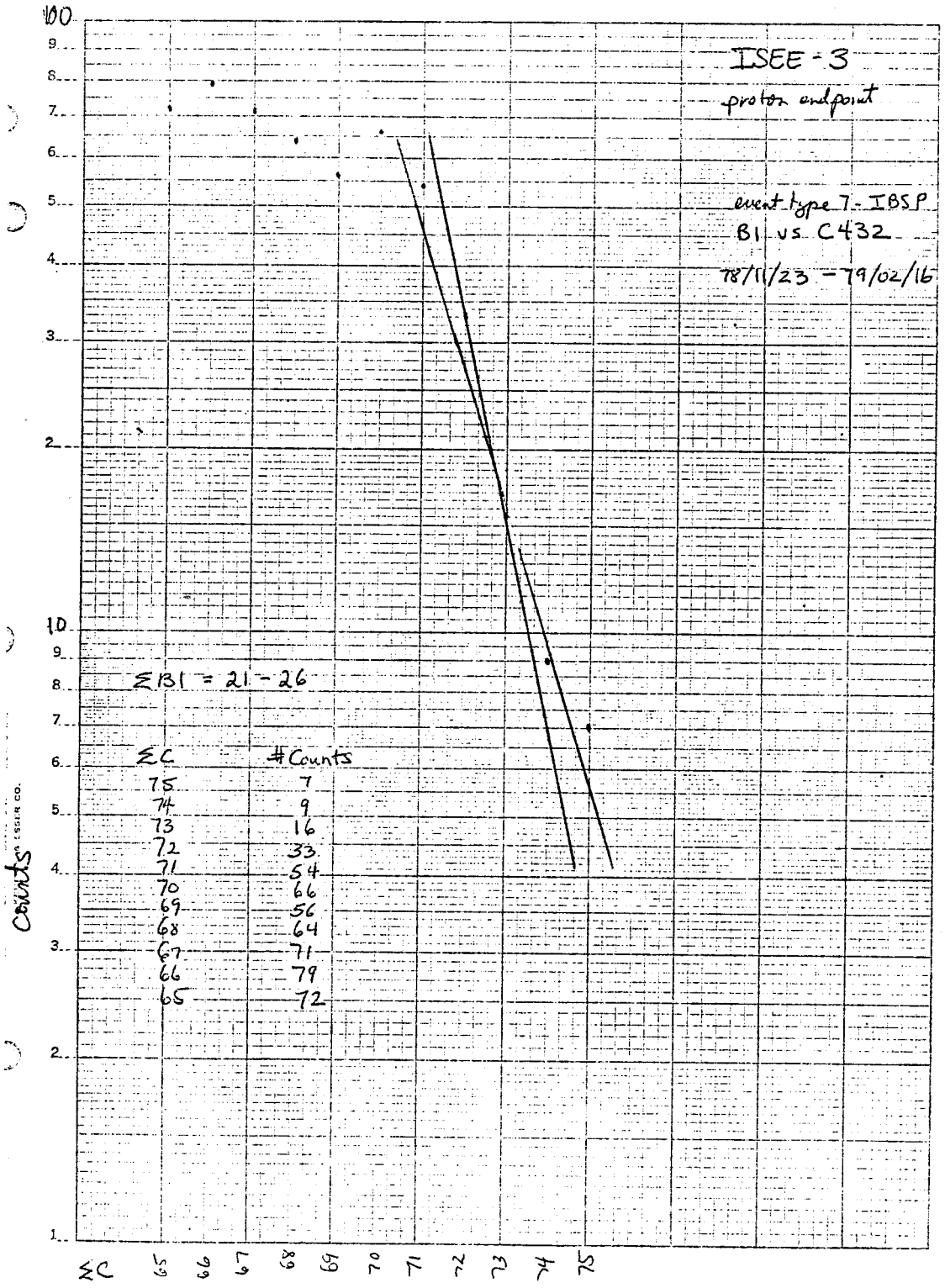

Figure 13. Total Counts across TRACK Plotted against Detector B1

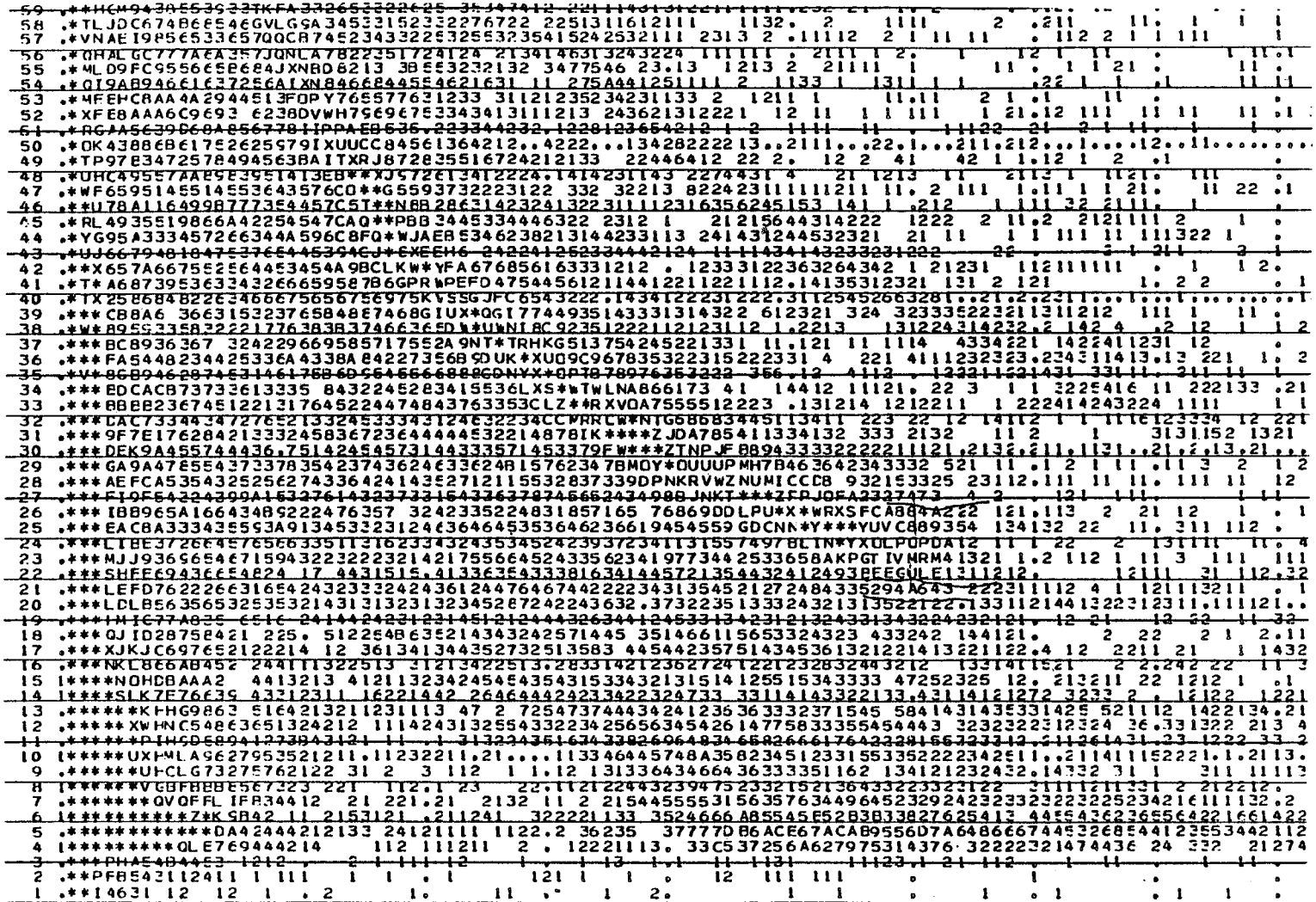

Figure 14. Endpoint Data for proton B2 vs C432 HET-I

26	15	12	10	8	8	4	10	2	2	2	-	1	2	
25	34	30	34	12	8	8	9	3	5	4	-	1	3	
24	33	24	21	25	24	25	13	10	1	2	-	1	1	
23	16	29	18	34	22	27	22	4	1	3	2	1	-	
22	11	14	14	16	30	21	14	1	3	1	1	2	1	
21	5	2	9	4	10	6	4	3	-	2	2	2	3	
20	1	3	5	2	2	1	2	2	-	1	3	3	1	
	66	67	68	69	70	71	72	73	74	75	76	77	78	

IBSP 7, B2 vs C432

78/11/23 79/02/16

Figure 15. Data from Mass Line End

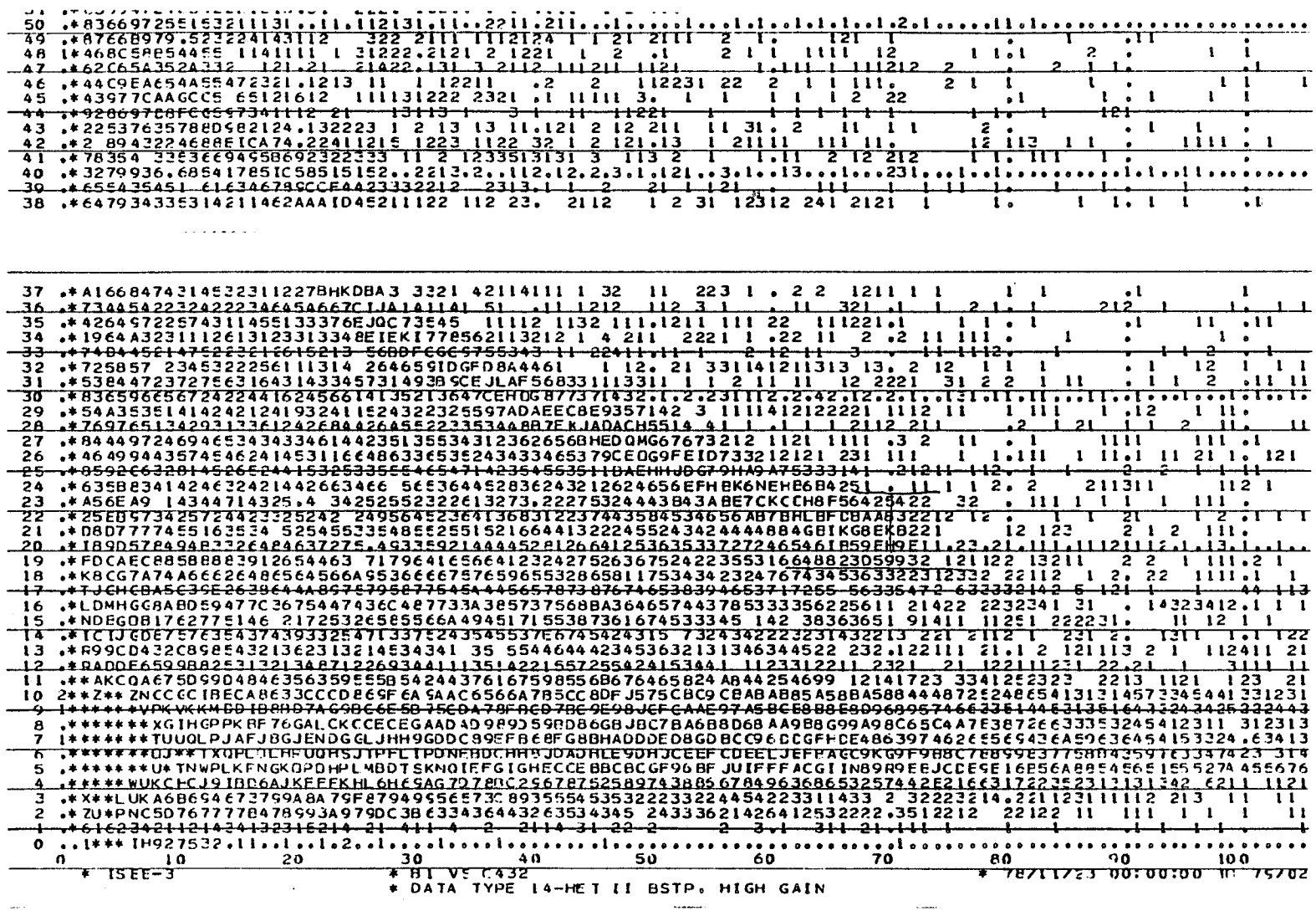

Figure 16. Endpoint Data for proton B1 vs C432 HET-II

Figure 17. Endpoint Data for proton B2 vs C432 HET-II

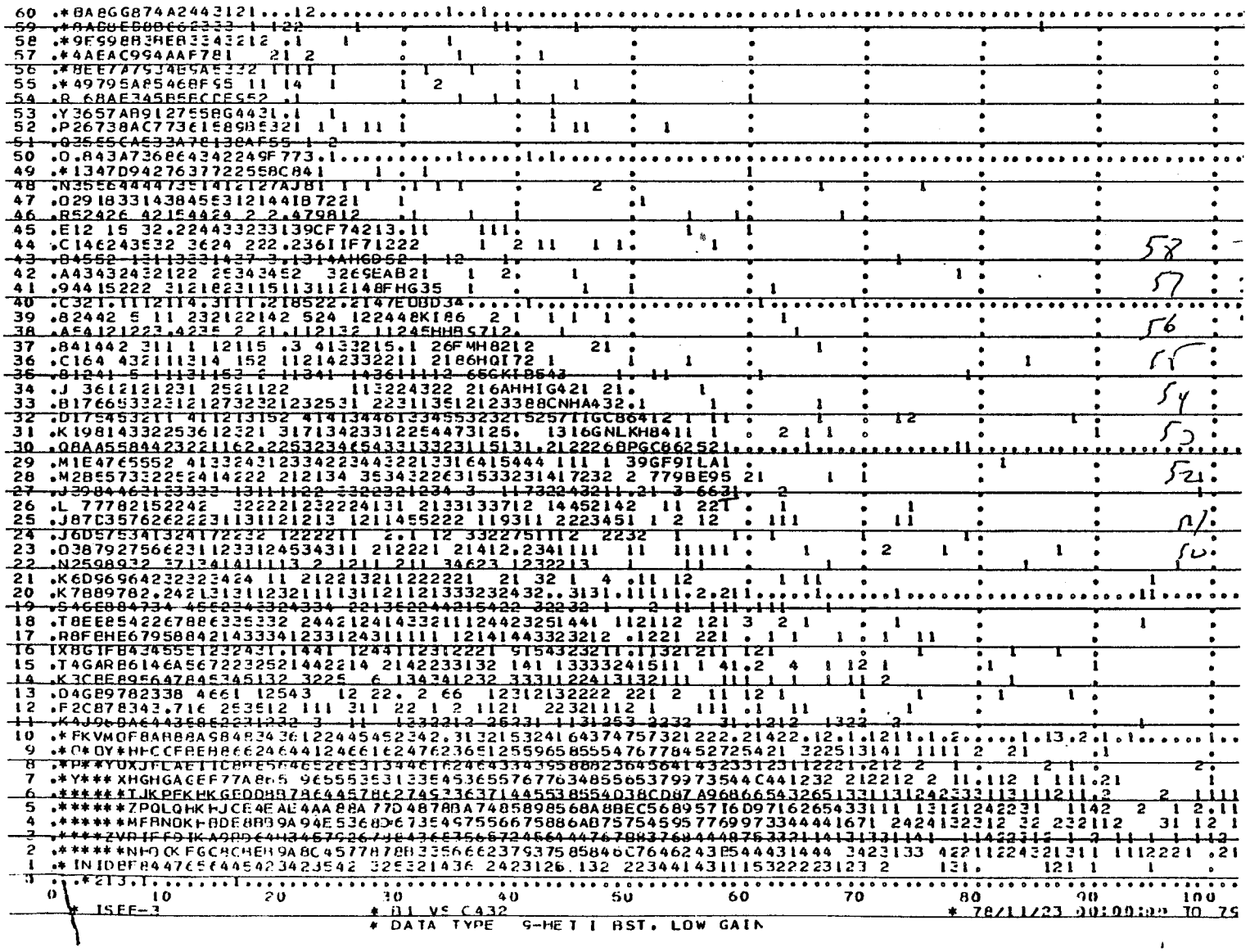

Figure 18. Endpoint Data for alpha B1 vs C432 HET-I low gain

33	10	4	3	2	-	1	-	-	-	-	-	-	1	-
32	18	16	12	8	6	4	1	2	-	1	-	-	1	1
31	6	16	23	21	20	17	8	4	1	1	-	1	-	-
30	2	2	6	11	25	16	12	8	6	2	5	2	1	-
29	1	-	1	-	3	9	16	15	9	18	21	10	1	-
28	2	3	2	-	2	-	7	7	9	11	14	9	5	-
27	3	2	1	1	-	2	1	-	3	-	6	6	3	1
26	5	2	1	4	2	-	-	1	1	-	2	2	1	-
	46	47	48	49	50	51	52	53	54	55	56	57	58	59

IBSP 9, B1 vs C432 low gain
78/11/23 79/02/16

Figure 19. Data from Mass Line End

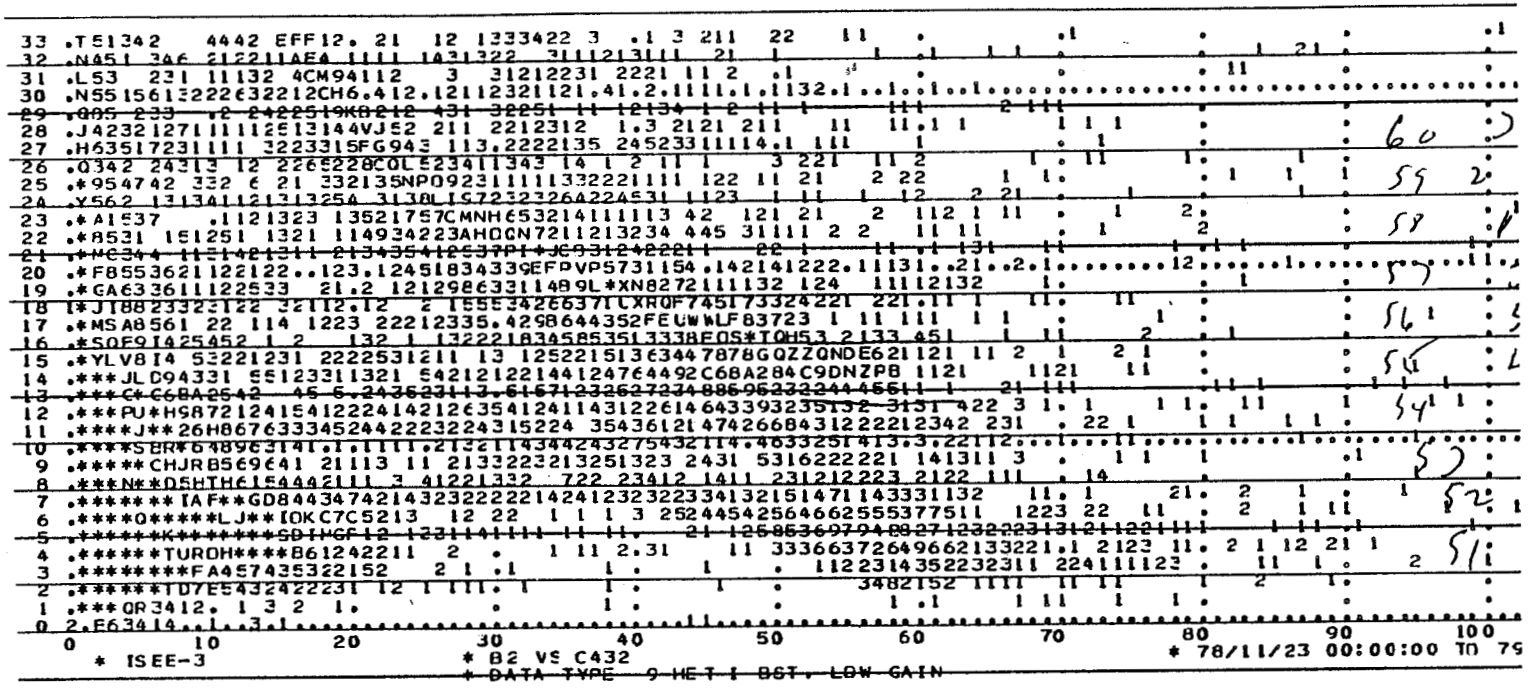

Figure 20. Endpoint Data for alpha B2 vs C432 - HET-I low gain

ISEE-3

18	3	3	2	4	2	2	1	-	2	2	1	-	1	1
17	3	7	2	3	-	1	-	1	1	-	1	1	1	-
16	29	26	17	5	3	-	2	1	3	3	-	4	5	1
15	16	26	35	35	26	23	13	14	6	2	1	1	2	1
14	2	8	4	12	9	13	23	35	25	11	-	1	1	2
13	5	2	3	2	2	4	4	4	5	5	1	1	-	1
12	9	3	2	3	5	1	3	2	-	3	1	3	1	-
11	6	6	8	4	3	1	2	2	2	2	1	2	3	4
	49	50	51	52	53	54	55	56	57	58	59	60	61	62

IBSP 9, B2 vs C432 low gain
78/11/23 79/02/16

Figure 21. Data from Mass Line End

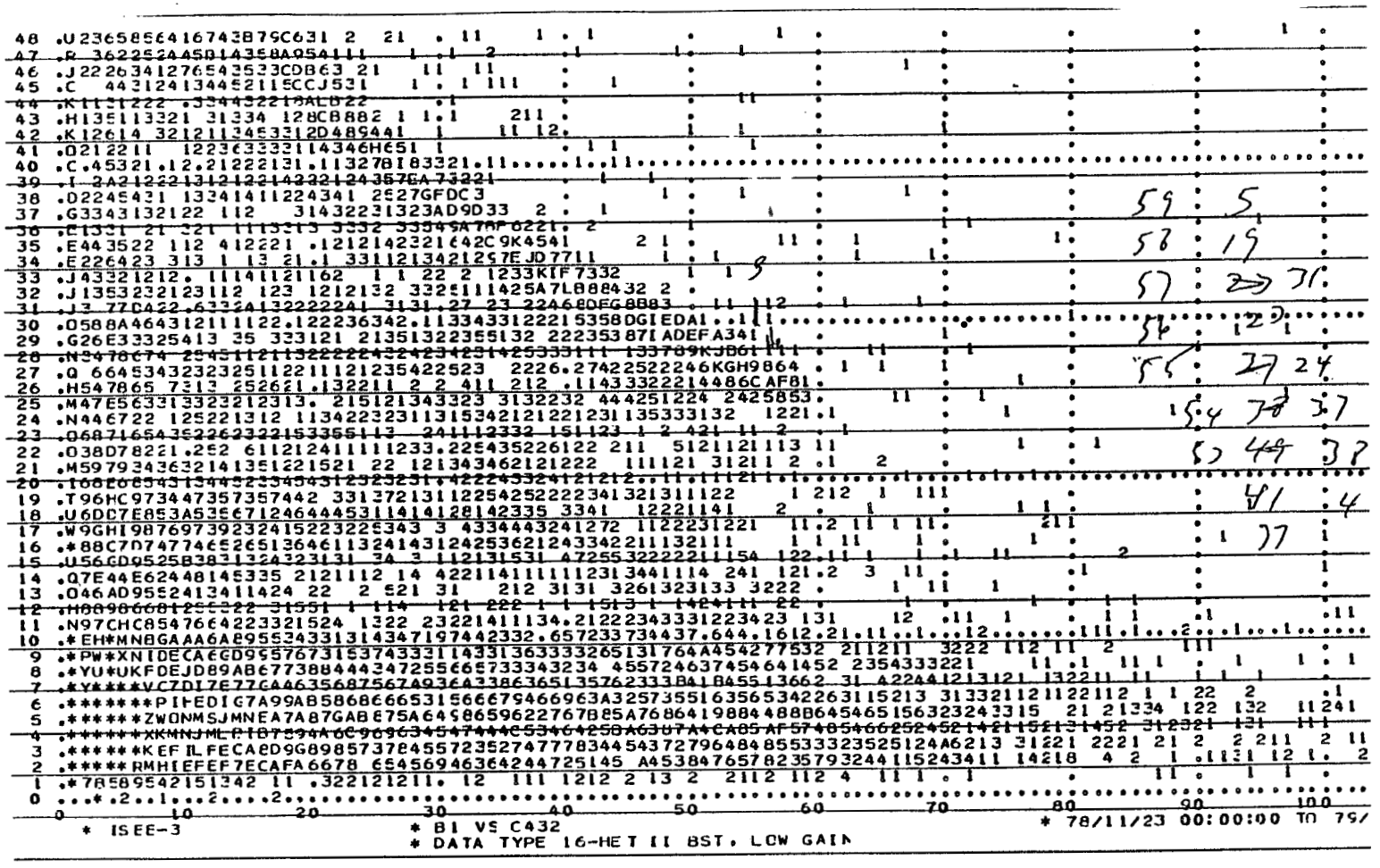

Figure 22. Endpoint Data for alpha B1 vs C432 HET-II low gain

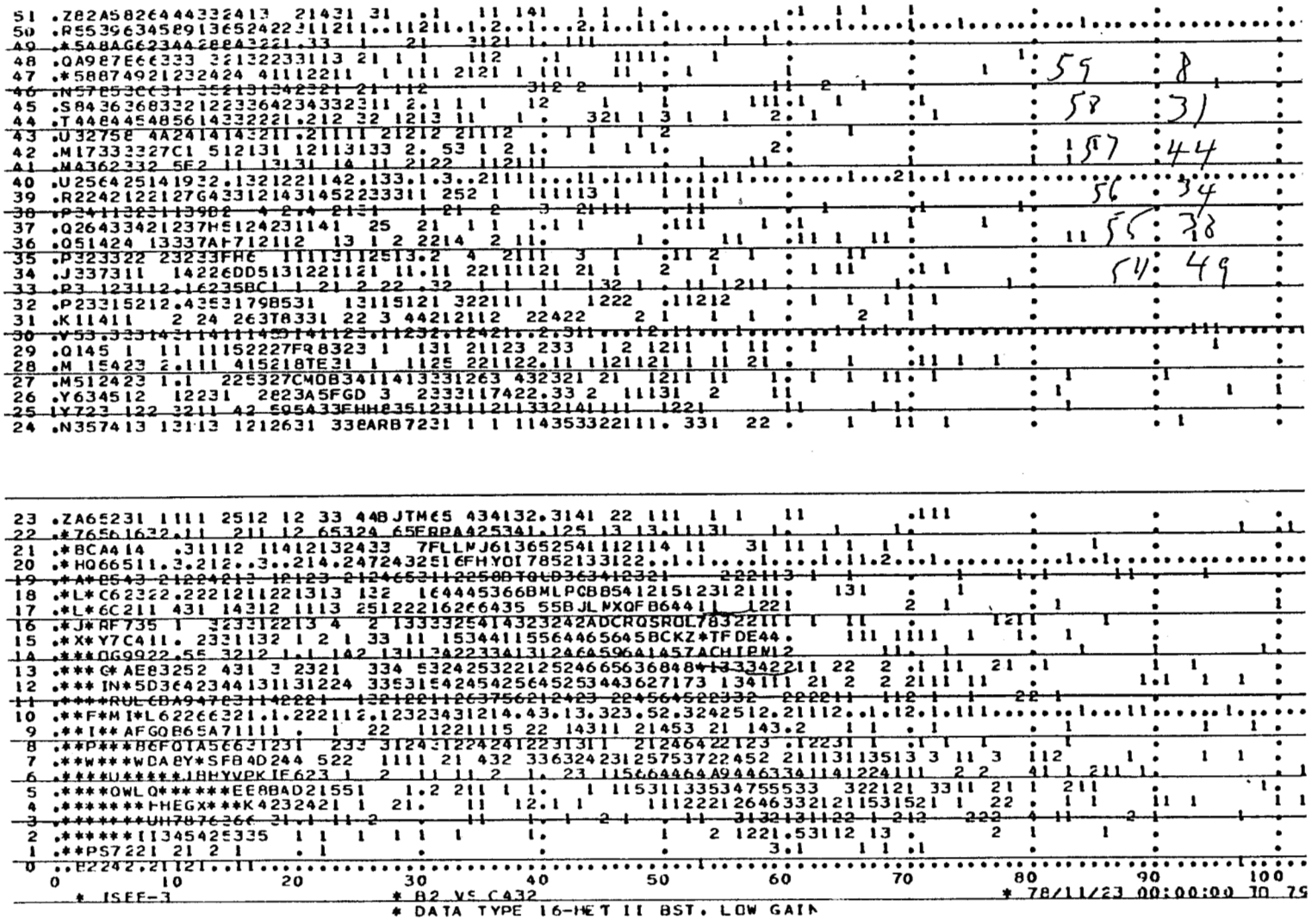

Figure 23. Endpoint Data for alpha B2 vs C432 HET-II low gain

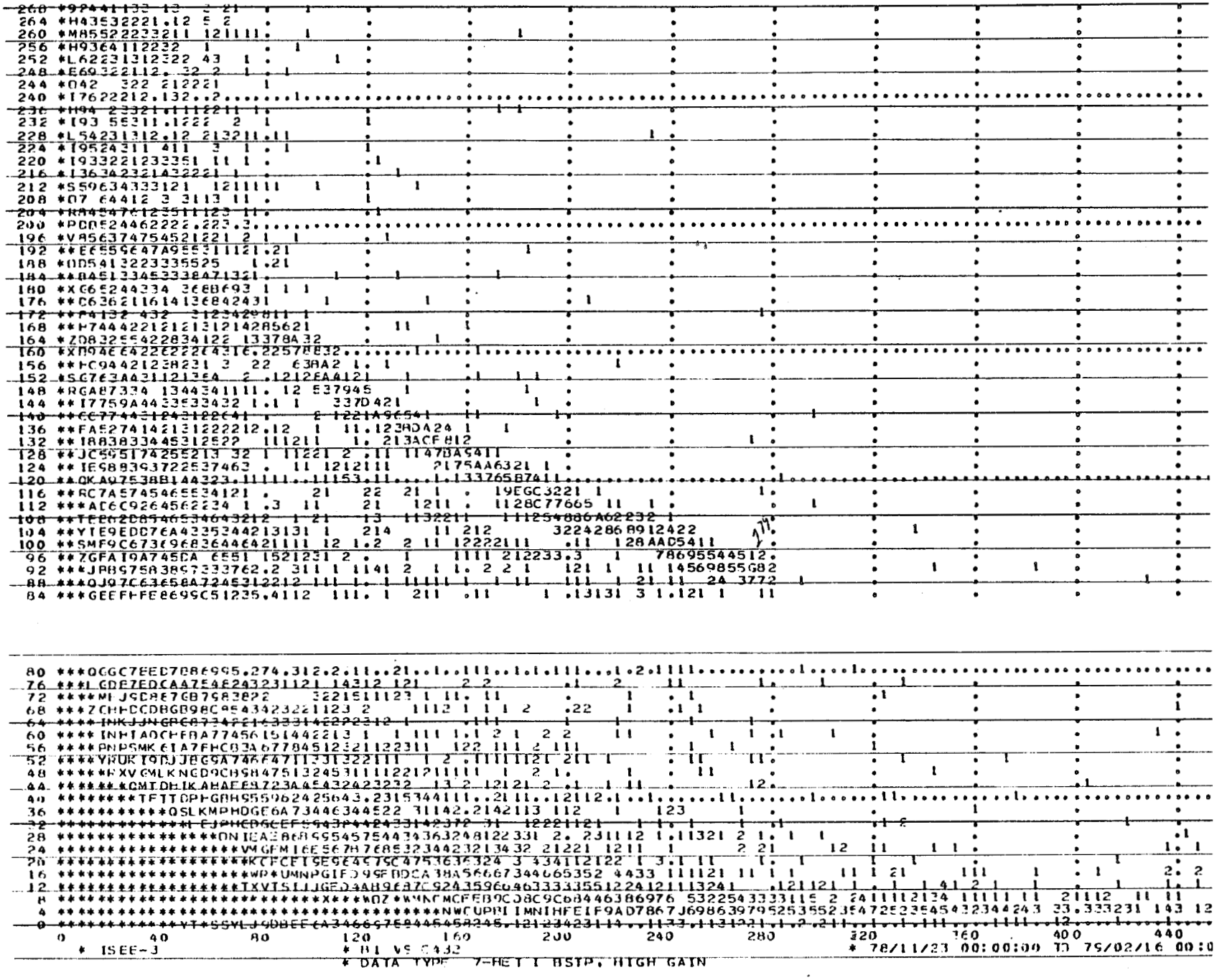

Figure 24. Endpoint Data f alpha B1 vs C432 HET-I

Figure 25. Endpoint Data for alpha B2 vs C432 HET-I

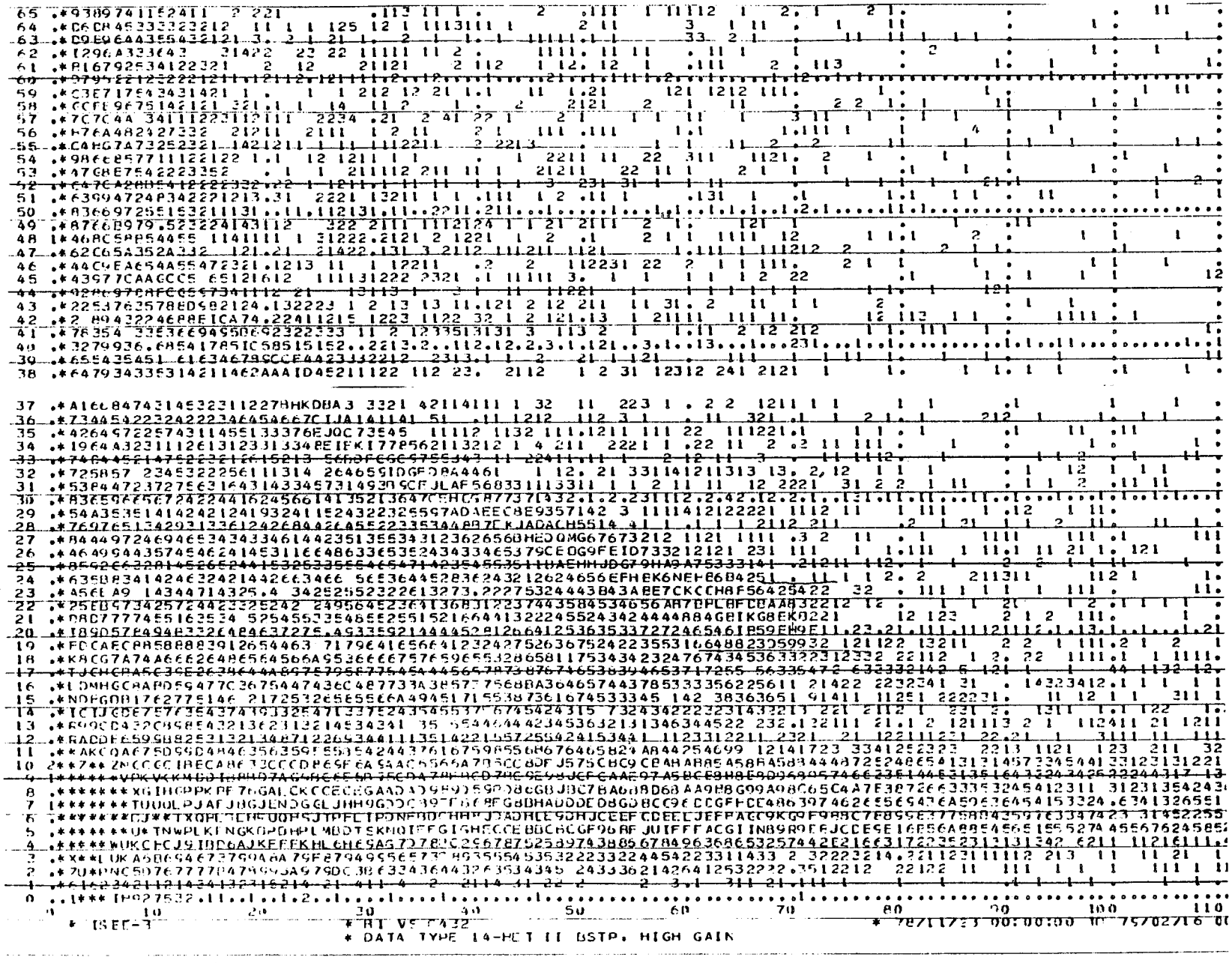

Figure 26. Endpoint Data for alpha B1 vs C432 HET-II

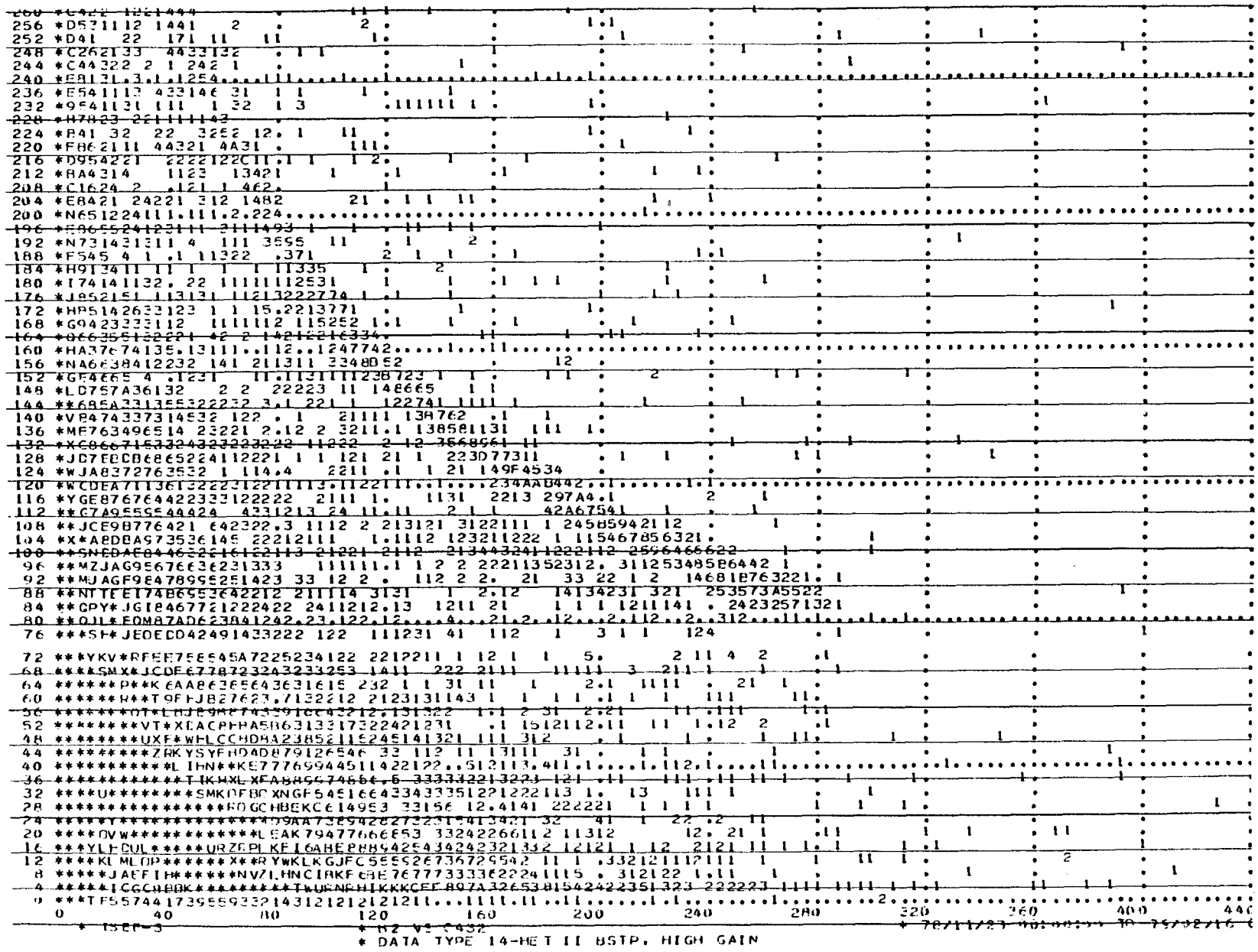

Figure 27. Endpoint Data for alpha B2 vs C432 HET-II

APPENDIX B - STOPPING PARTICLE WORK - RESPONSE DOCUMENTATION

The 2 and 3 dimensional stopping particle responses (summarized above in Sections 4.3 and 4.4) were made with the programs TESTA and BOXGEN (AUTOBOX version: see Volume 1, Appendix C, page 129 of this Document). As mentioned in the introduction to this volume, Dr. Don Reames generated these responses.

TESTA was run most often with a 5% energy increment parameter value, and all other program defaults. A copy of that program is included in the computer printout book II of the ISEE CALIBRATION documentation. The detector description files used as input to TESTA are shown in Tables 16 through 21 . These detector descriptions are located on the PDP 11/70 in the following data files:

[200,105]IH1LOZ.DET
[200,105]IH2LOZ.DET
[200,105]IH1HIZ.DET
[200,105]IH2HIZ.DET
[200,105]IH1HG2D.DET
[200,105]IH2HG2D.DET

The program BOXGEN (or AUTOBOX) was used to make computer TRACKS. The box-spread and overlay priority parameters were used to help define the width and location of the TRACKS. An iterative process was used, in which the shape of each particle's computer TRACK was made to give the best overlay of the actual mass line. Summary printouts of these runs are shown in Tables 22 through 24 . The complete output from these BOXGEN (AUTOBOX) runs is located in the documentation book II mentioned above. Notice that the 2-dimensional stopping responses of Table 22 replace the